

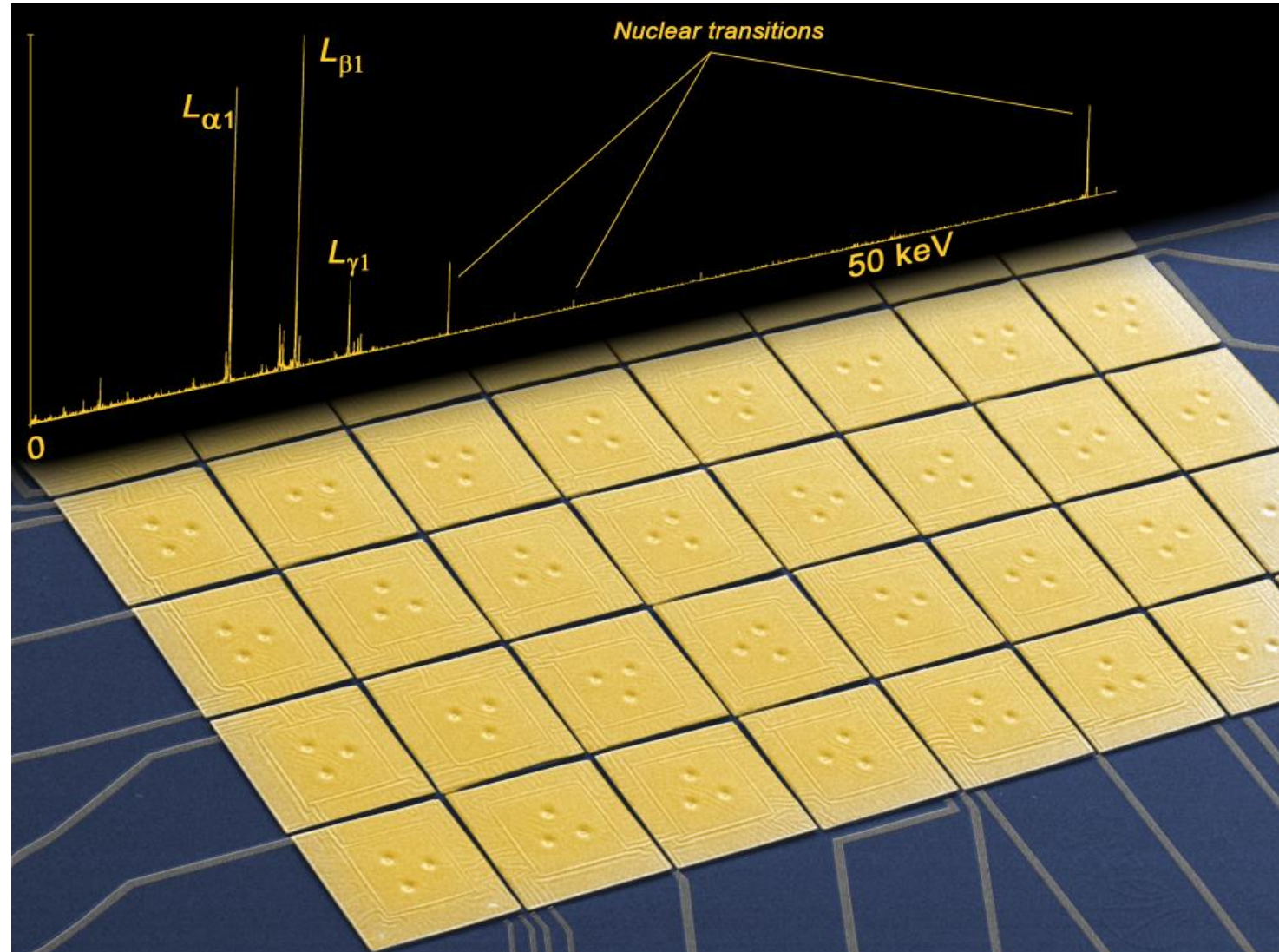
Metallic Magnetic Calorimeters for muonic atoms spectroscopy

A. Abeln, E. Biedert, T. E. Cocolios,
O. Eizenberg, C. Enss, A. Fleischmann,
L. Gastaldo, C. Godinho, M. Heines,
D. Hengstler, P. Indelicato, D. Kreuzberger,
K. Kirch, A. Knecht, J. Machado, B. Ohayon,
N. Paul, R. Pohl, A. Reifenberger,
K. von Schoeler, A. Striebel, D. Unger,
S. M. Vogiatzi, F. Wauters, J. Wendel and
P. Wiedemann

— for the QUARTET Collaboration



UNIVERSITÄT
HEIDELBERG
ZUKUNFT
SEIT 1386



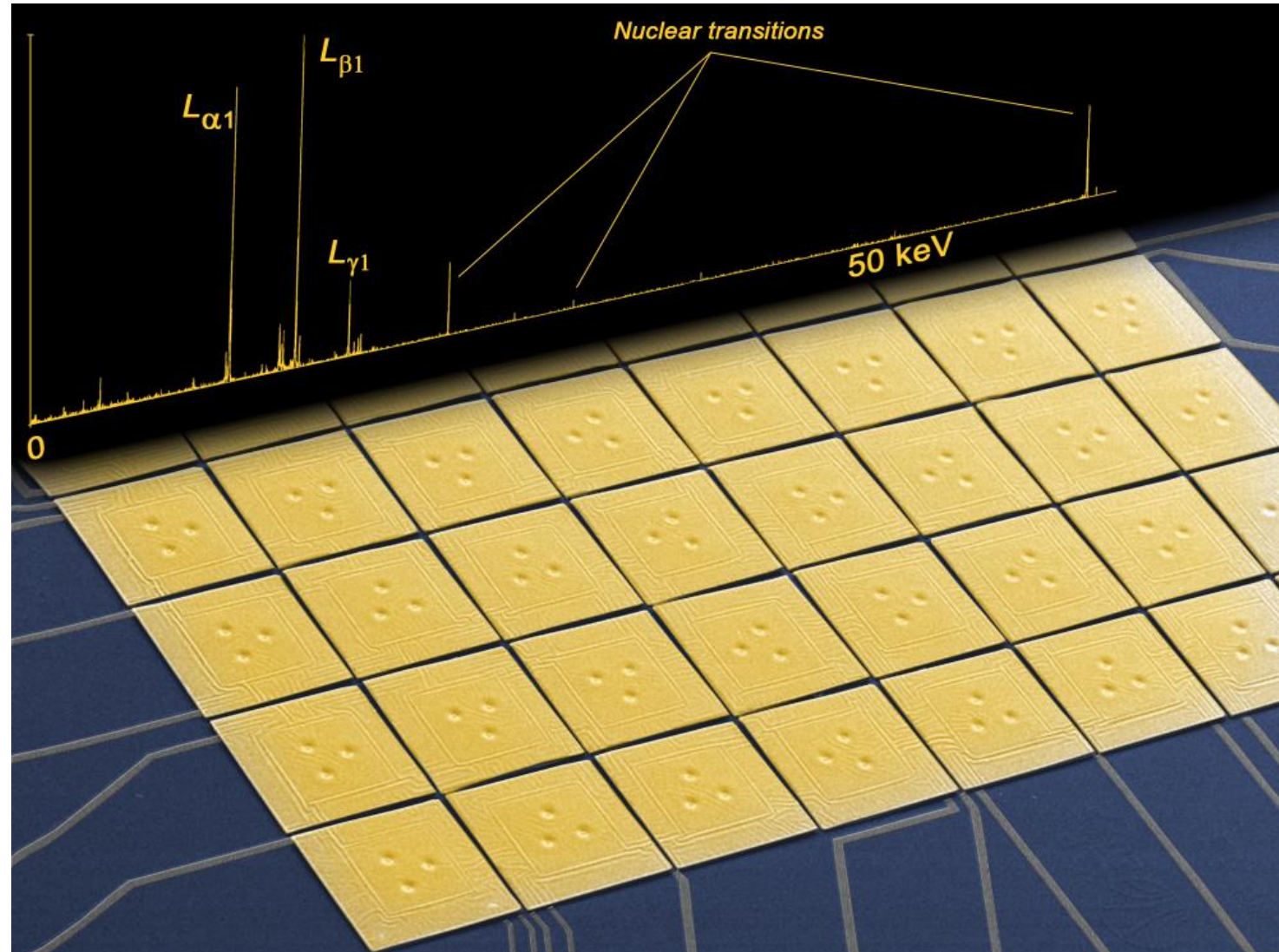
Metallic Magnetic Calorimeters for muonic atoms spectroscopy

A. Abeln, E. Biedert, T. E. Cocolios,
O. Eizenberg, C. Enss, A. Fleischmann,
L. Gastaldo, C. Godinho, M. Heines,
D. Hengstler, P. Indelicato, D. Kreuzberger,
K. Kirch, A. Knecht, J. Machado, B. Ohayon,
N. Paul, R. Pohl, A. Reifenberger,
K. von Schoeler, A. Striebel, D. Unger,
S. M. Vogiatzi, F. Wauters, J. Wendel and
P. Wiedemann

— for the QUARTET Collaboration

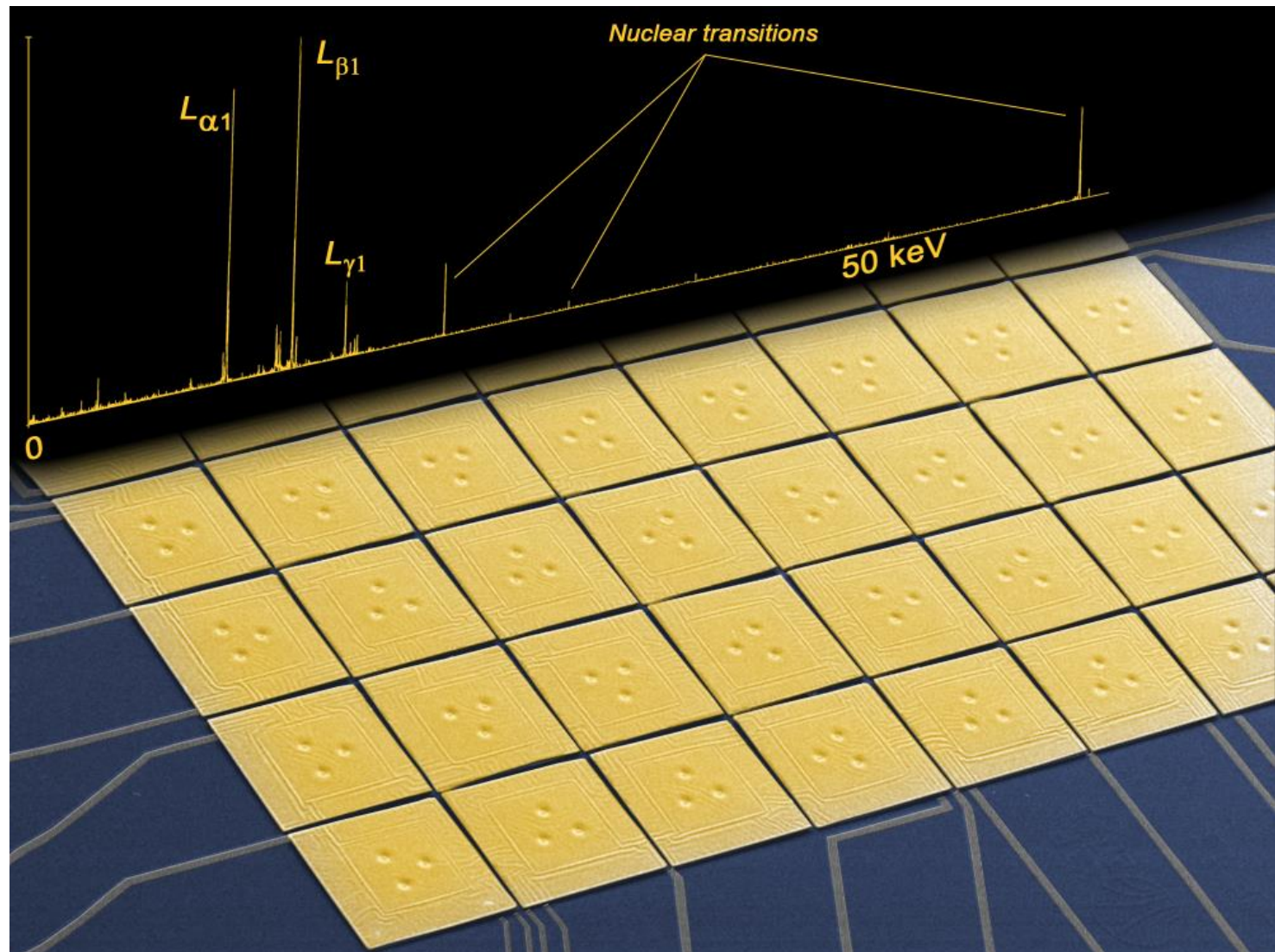


UNIVERSITÄT
HEIDELBERG
ZUKUNFT
SEIT 1386



Outlook

- Metallic Magnetic Calorimeters (MMCs)
- MMCs for x-ray spectroscopy
- QUARTET



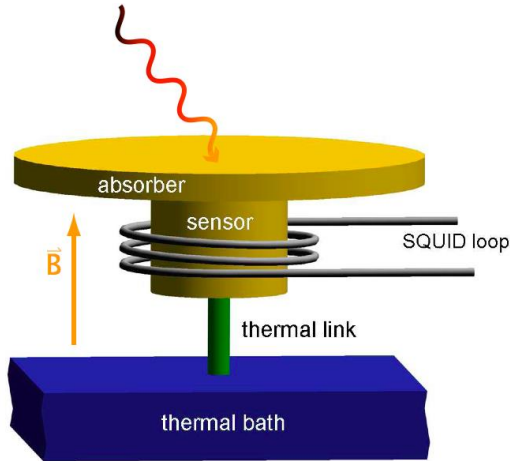
Metallic Magnetic Calorimeters

A.Fleischmann, C. Enss and G. M. Seidel,
Topics in Applied Physics **99** (2005) 63

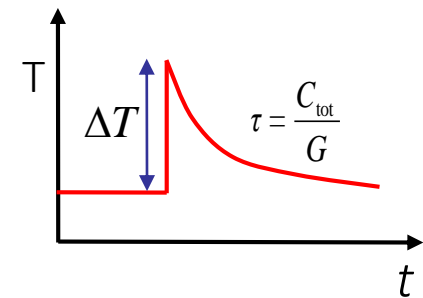
A.Fleischmann et al.,
AIP Conf. Proc. **1185** (2009) 571

Paramagnetic temperature sensor

Dilute alloy Au:Er or Ag:Er (Er concentration: a few hundred ppm)



$$\Delta T \cong \frac{E}{C_{\text{tot}}}$$



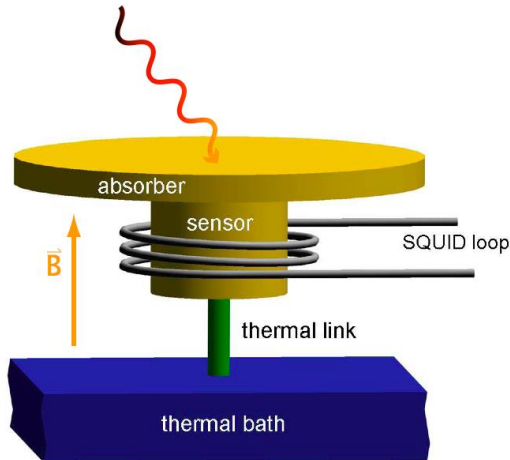
Metallic Magnetic Calorimeters

A.Fleischmann, C. Enss and G. M. Seidel,
Topics in Applied Physics **99** (2005) 63

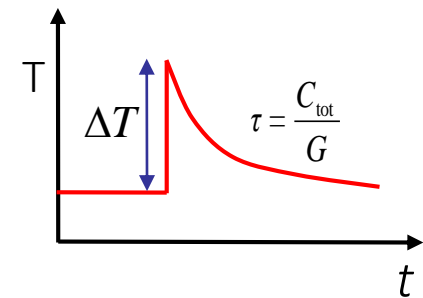
A.Fleischmann et al.,
AIP Conf. Proc. **1185** (2009) 571

Paramagnetic temperature sensor

Dilute alloy Au:Er or Ag:Er (Er concentration: a few hundred ppm)



$$\Delta T \cong \frac{E}{C_{\text{tot}}} \xrightarrow{\text{MMC}} \Delta \Phi_s \propto \frac{\partial M}{\partial T} \Delta T \rightarrow \Delta \Phi_s \propto \frac{\partial M}{\partial T} \frac{E}{C_{\text{tot}}}$$



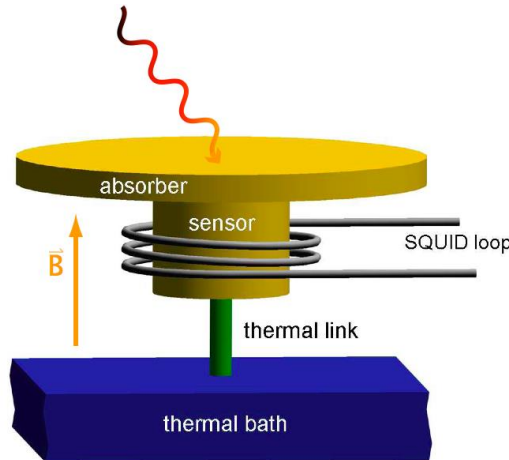
Metallic Magnetic Calorimeters

A.Fleischmann, C. Enss and G. M. Seidel,
Topics in Applied Physics **99** (2005) 63

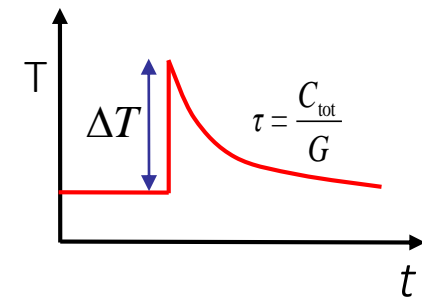
A.Fleischmann et al.,
AIP Conf. Proc. **1185** (2009) 571

Paramagnetic temperature sensor

Dilute alloy Au:Er or Ag:Er (Er concentration: a few hundred ppm)

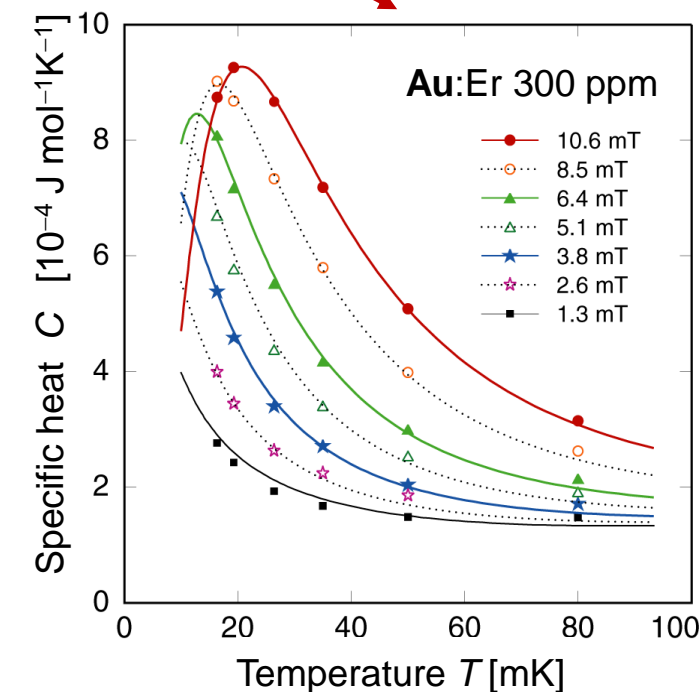
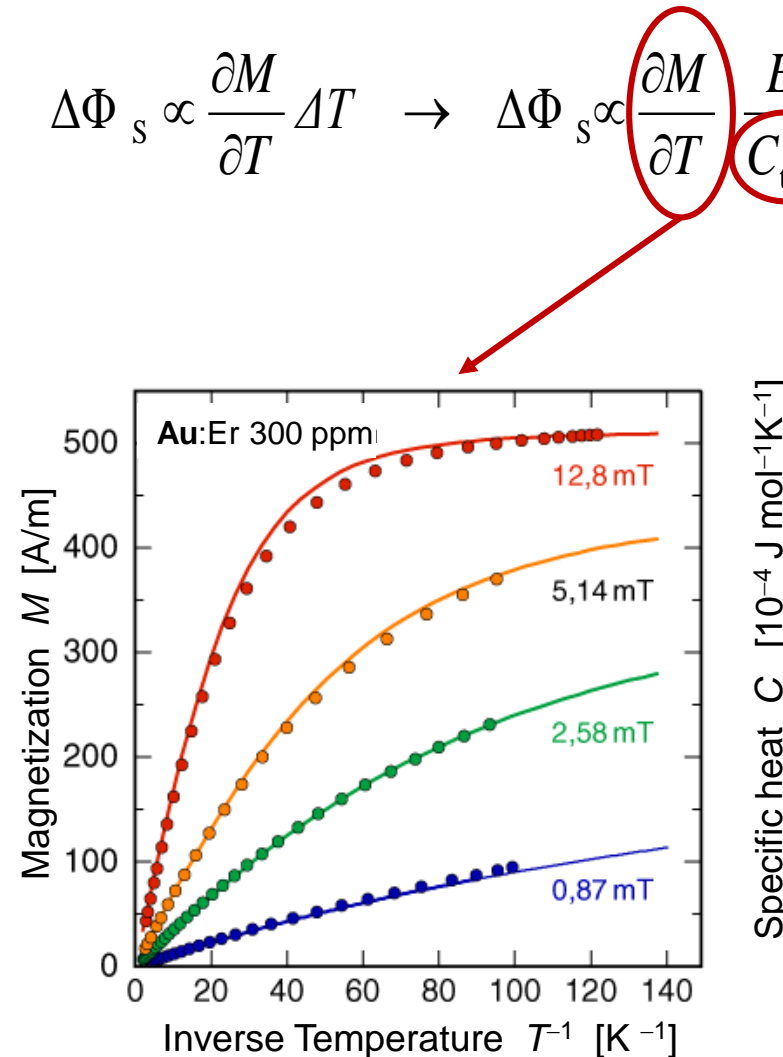


$$\Delta T \approx \frac{E}{C_{\text{tot}}} \xrightarrow{\text{MMC}}$$



Very good agreement between data and theoretical expectation for interacting spin system

Optimization of detector geometries for different applications



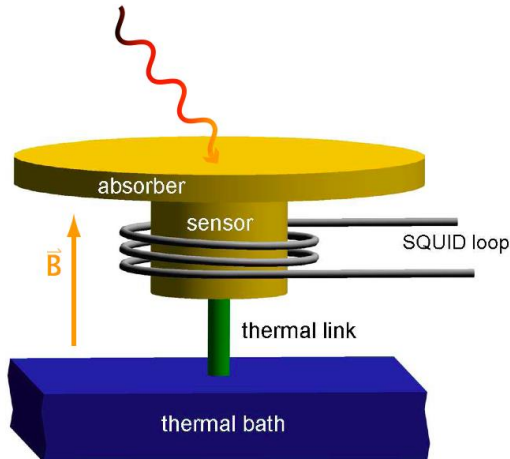
Metallic Magnetic Calorimeters

A.Fleischmann, C. Enss and G. M. Seidel,
Topics in Applied Physics **99** (2005) 63

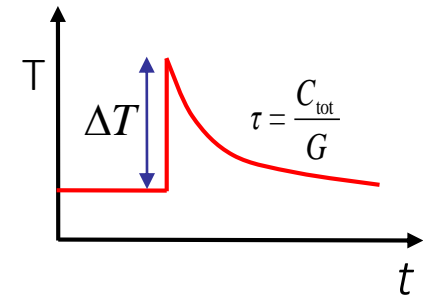
A.Fleischmann et al.,
AIP Conf. Proc. **1185** (2009) 571

Paramagnetic temperature sensor

Dilute alloy Au:Er or Ag:Er (Er concentration: a few hundred ppm)

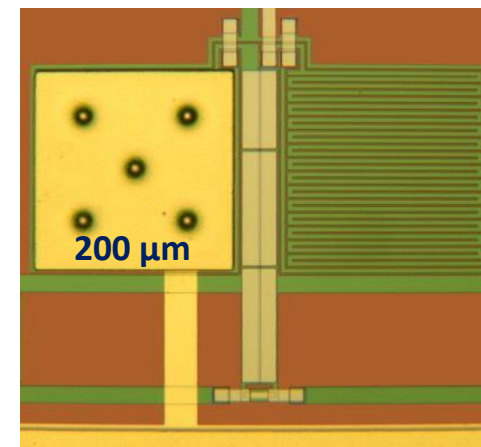
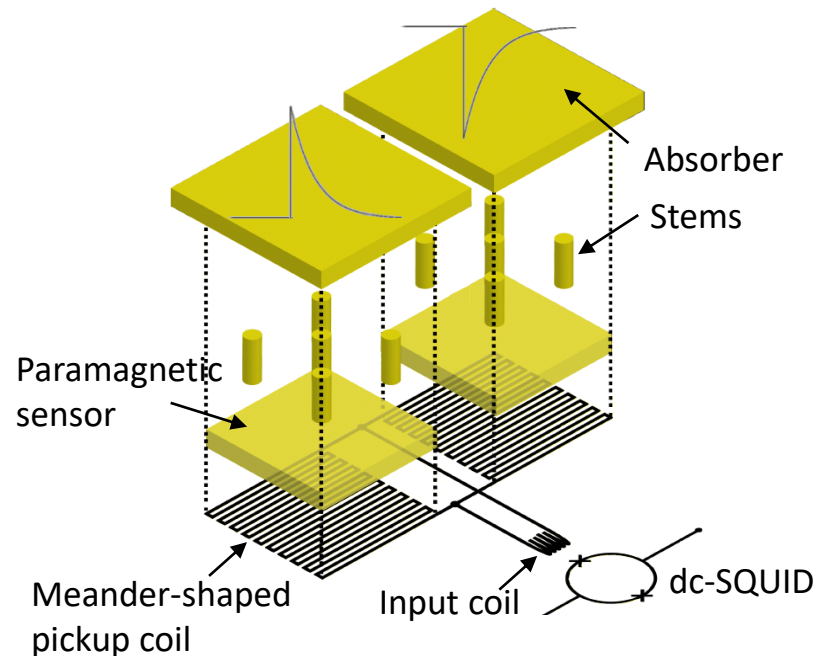


$$\Delta T \cong \frac{E}{C_{\text{tot}}} \xrightarrow{\text{MMC}} \Delta \Phi_s \propto \frac{\partial M}{\partial T} \Delta T \rightarrow \Delta \Phi_s \propto \frac{\partial M}{\partial T} \frac{E}{C_{\text{tot}}}$$



Very good agreement between data and theoretical expectation for interacting spin system

Optimization of detector geometries
for different applications

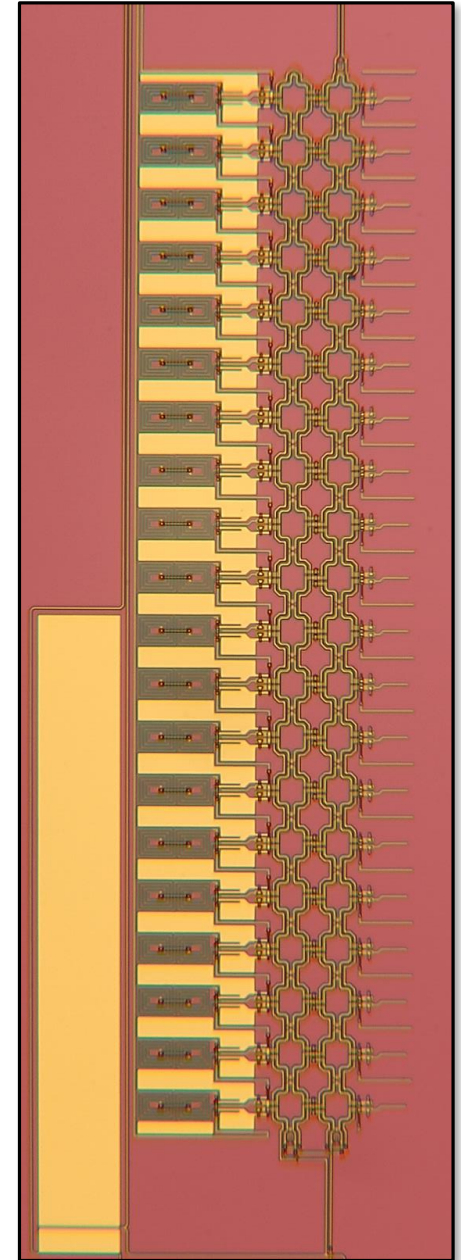
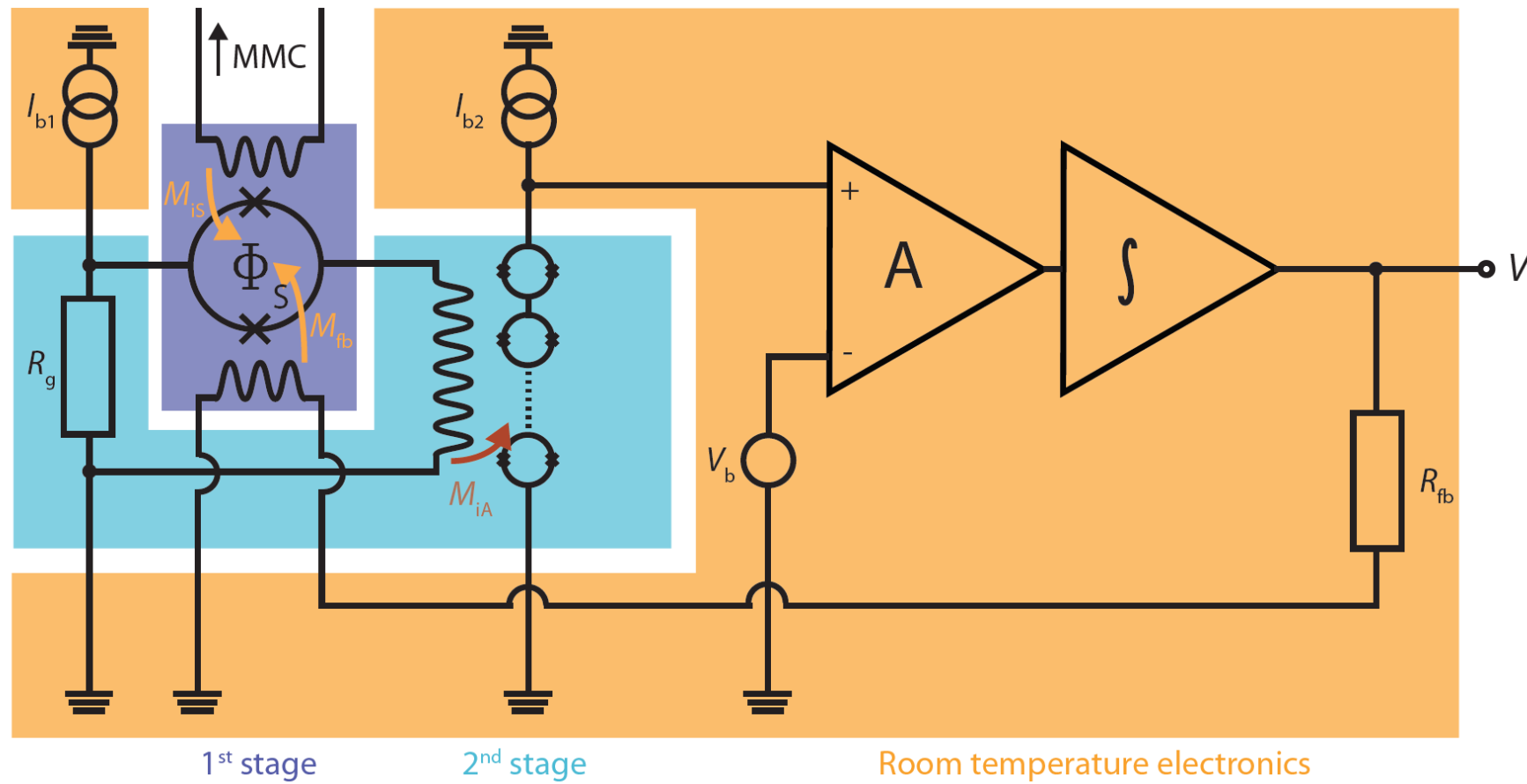


MMC readout

Two-stage dc-SQUID readout with flux-locked loop

low noise

small power dissipation on detector SQUID chip (voltage bias 1st stage)



In house produced SQUID array

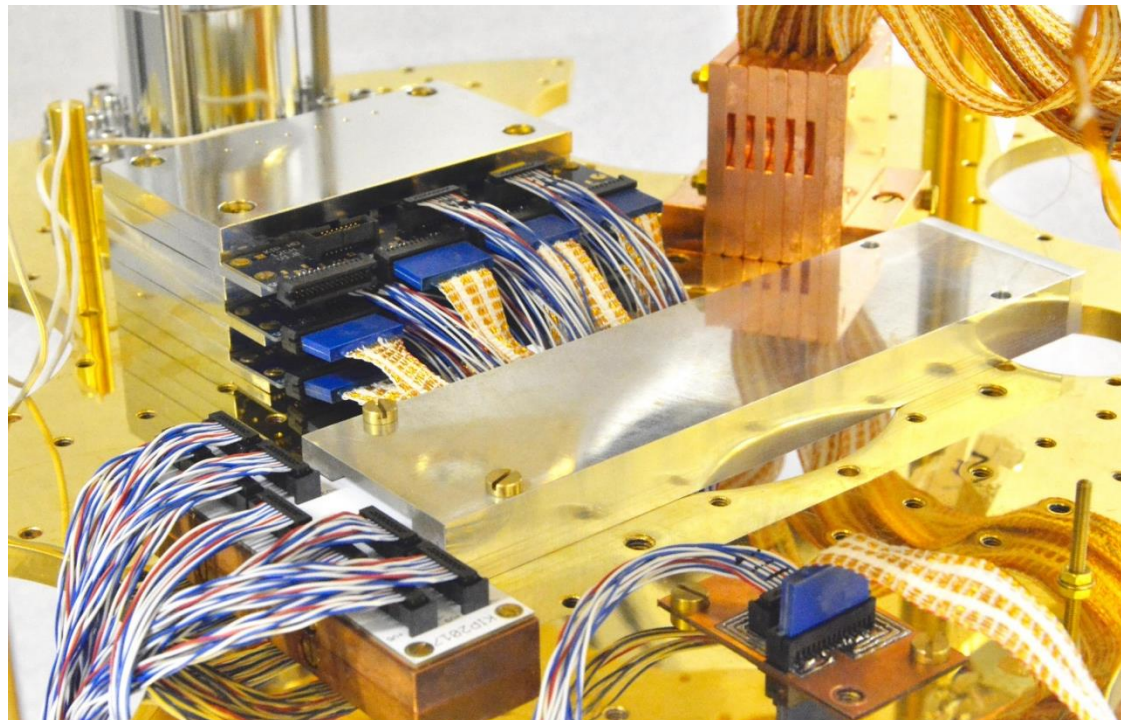
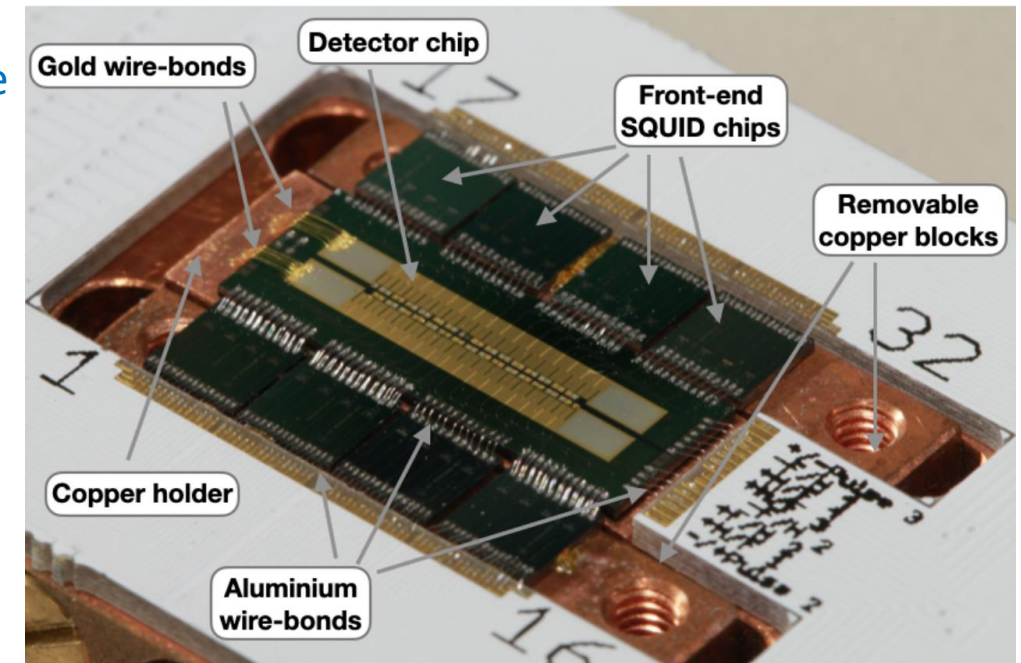
MMC readout



Amplifier module

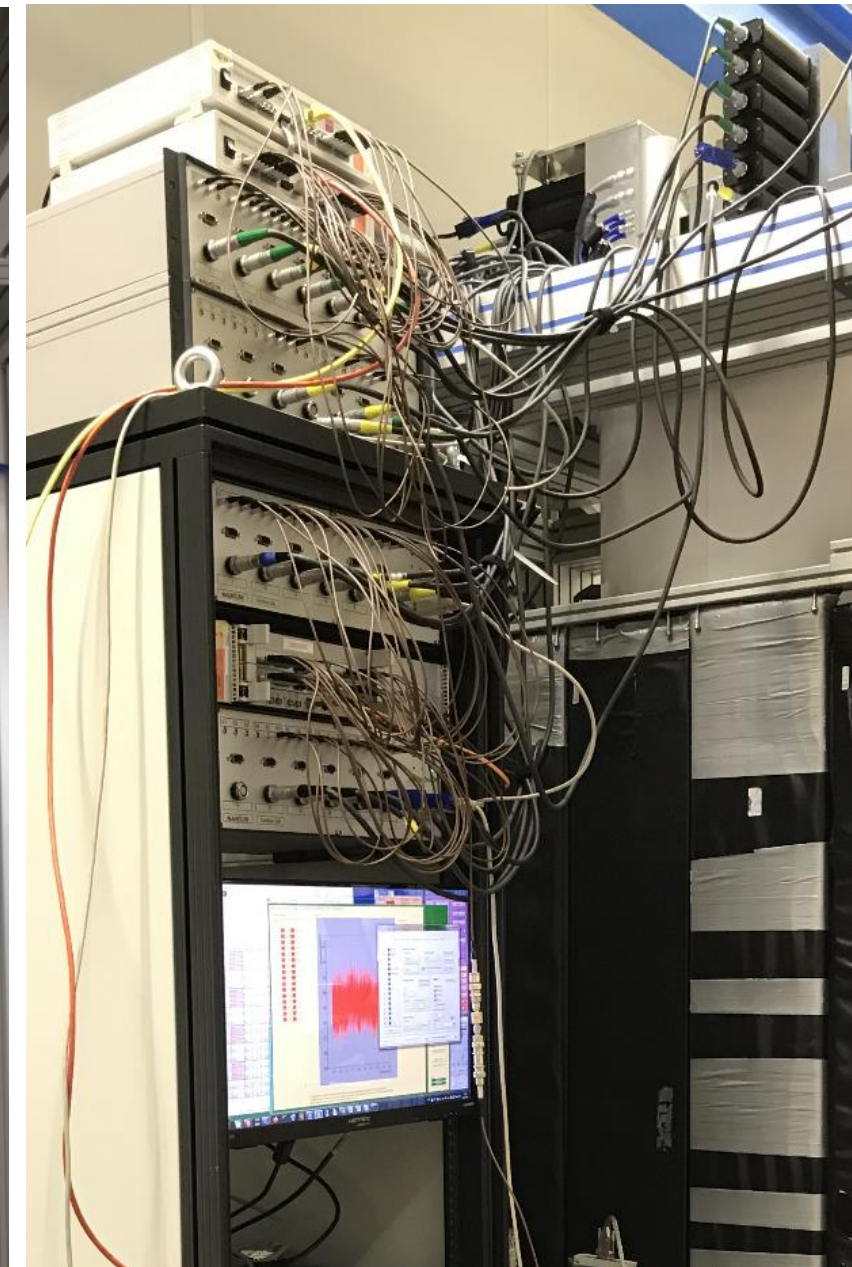
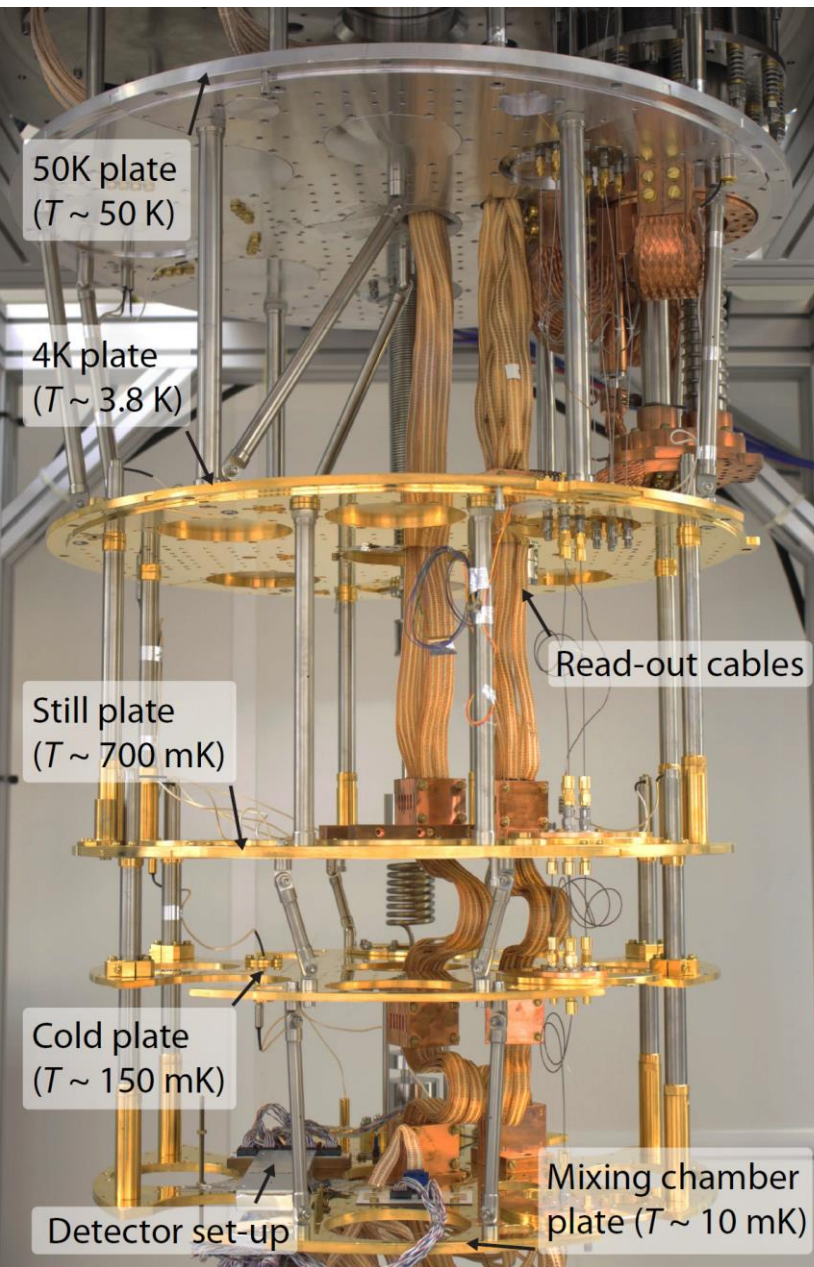
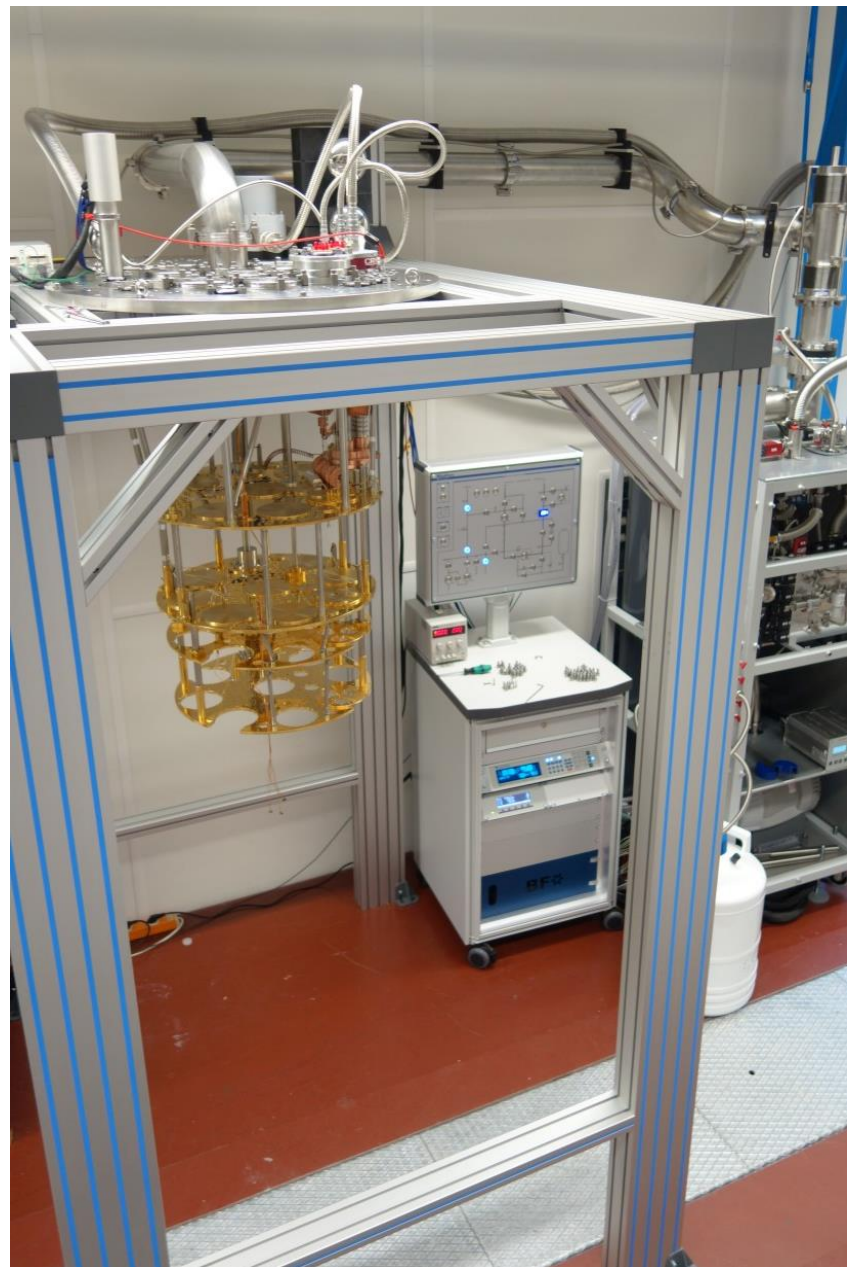


Detector module

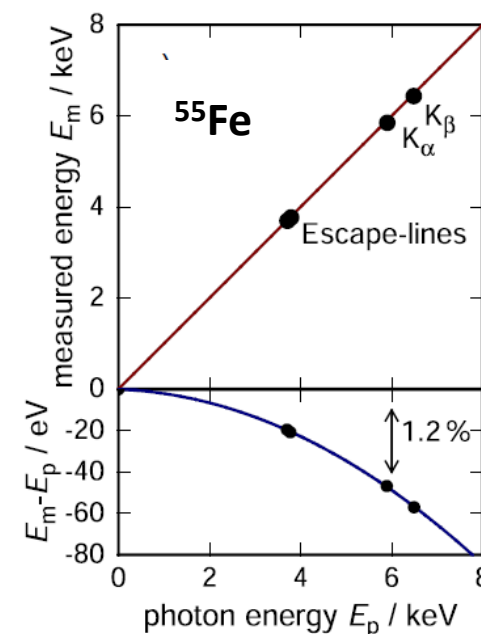
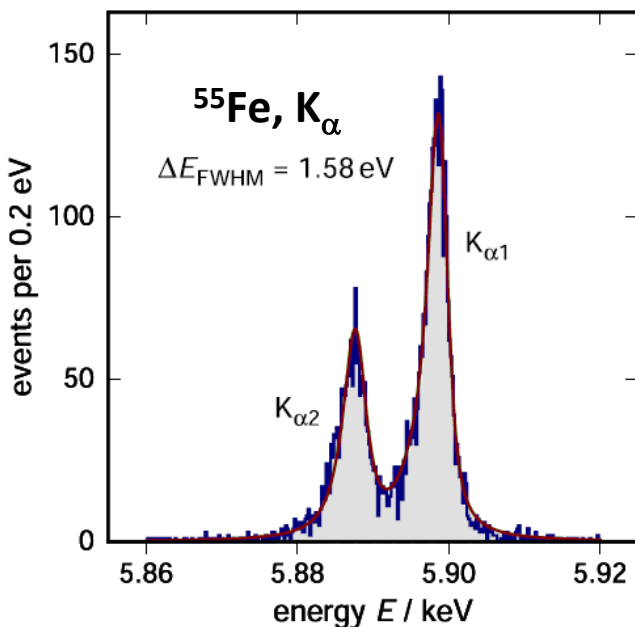
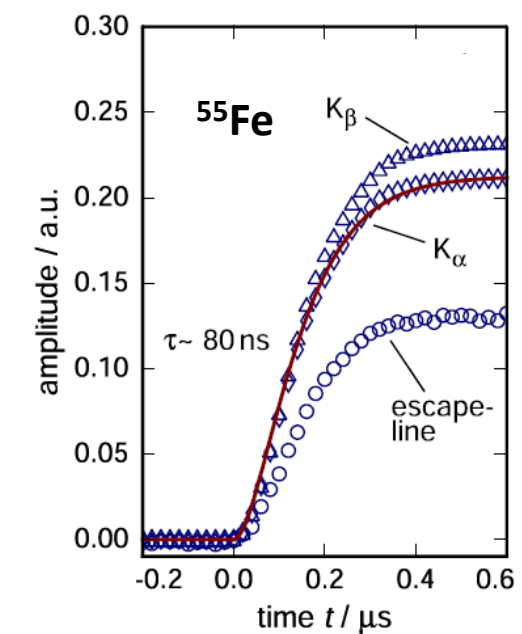


Detector and amplifier module
mounted on the
mixing chamber plate

MMC readout



Performance



Fast risetime

→ Reduction un-resolved pile-up

Extremely good energy resolution

→ identification of small structures

Excellent linearity

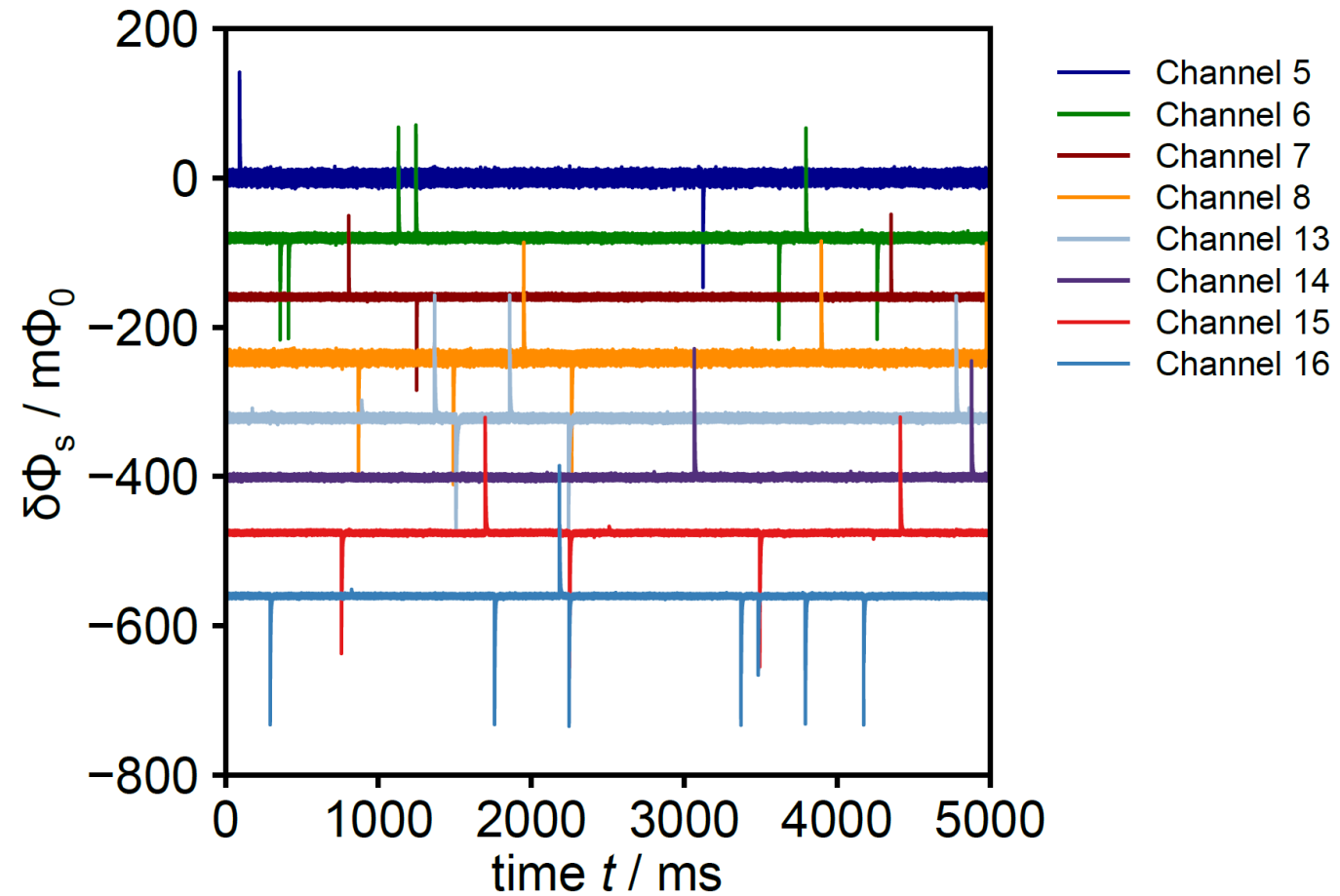
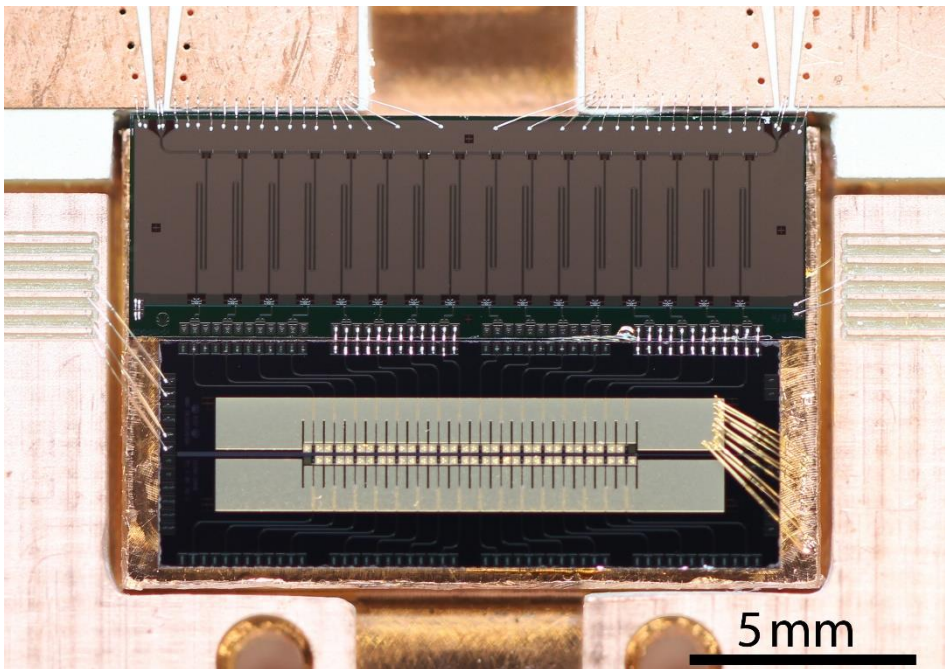
→ precise definition of the energy scale

MMC readout – Multiplexing R&D

Microwave SQUID multiplexing

Single HEMT amplifier and 2 coaxes
to read out **100 - 1000** detectors

- Successful characterization of first prototypes with external ^{55}Fe
→ **Very promising results:**
8 channels (16 pixels)



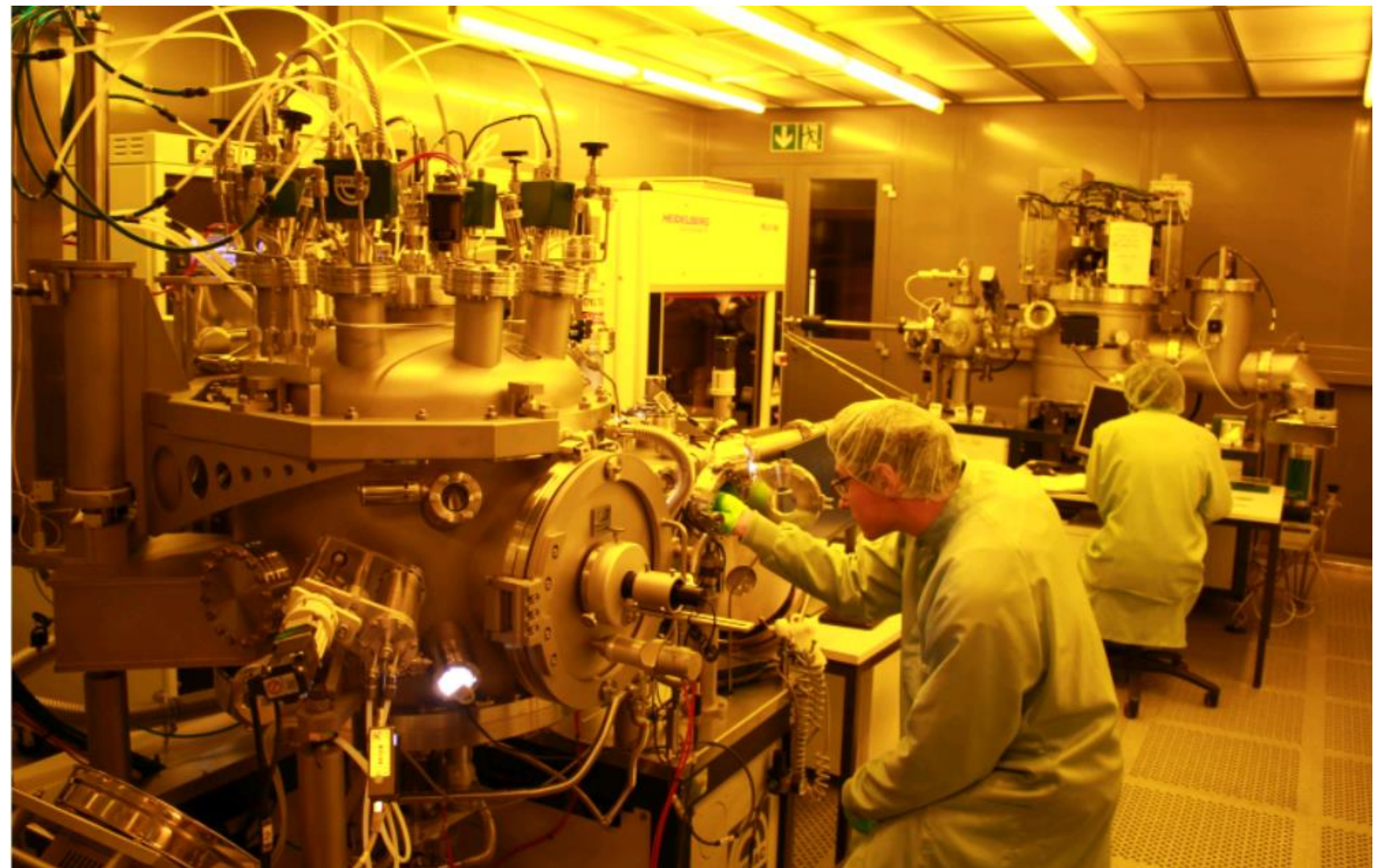
Energy resolution **below 10 eV FWHM** has been reached

MMC fabrication

40 m² Cleanroom class 100
at Kirchhoff Institute for Physics

Wet bench
Chemistry bench
Maskless aligner
UHV sputtering system
Dry etching system

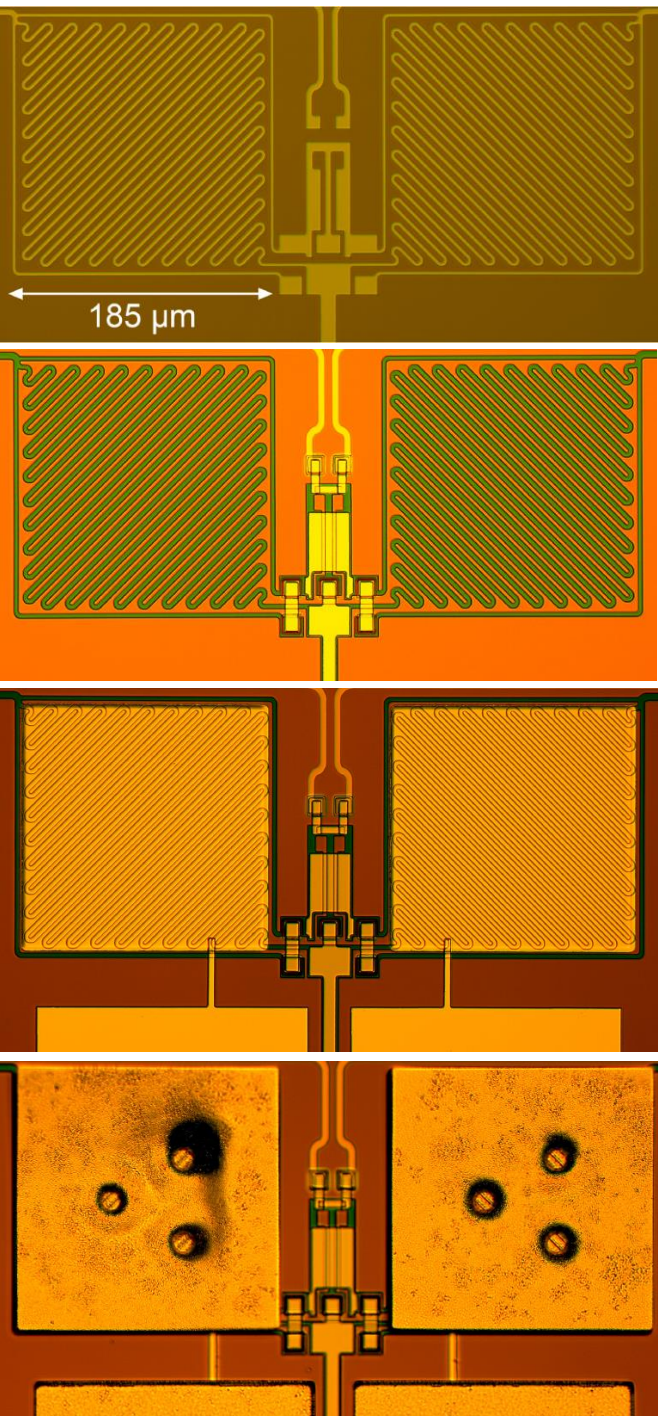
- Flexibility in design and fabrication
- Reliable processes for thin films
- Production of MMC array and superconducting electronics

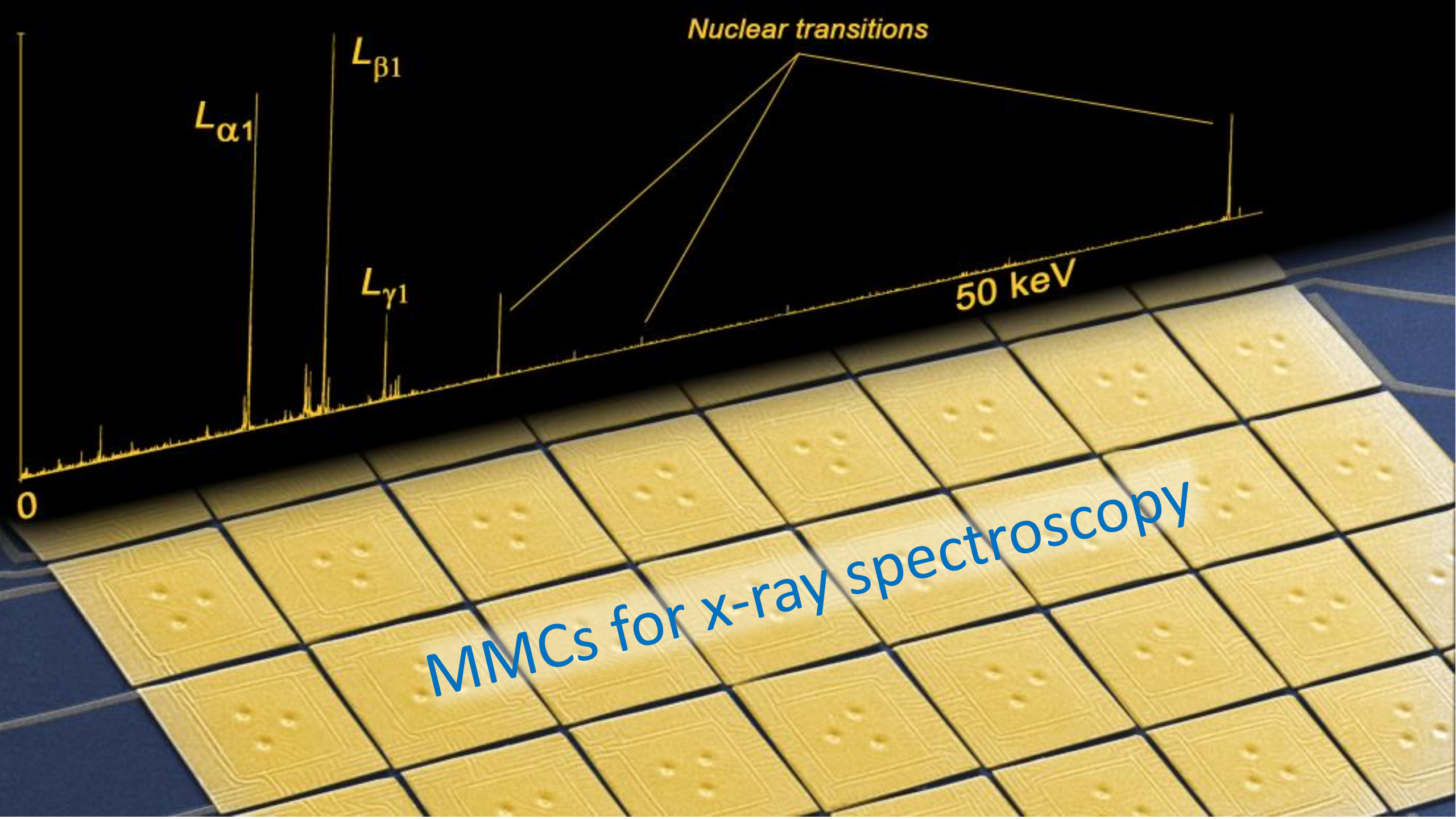


MMC fabrication

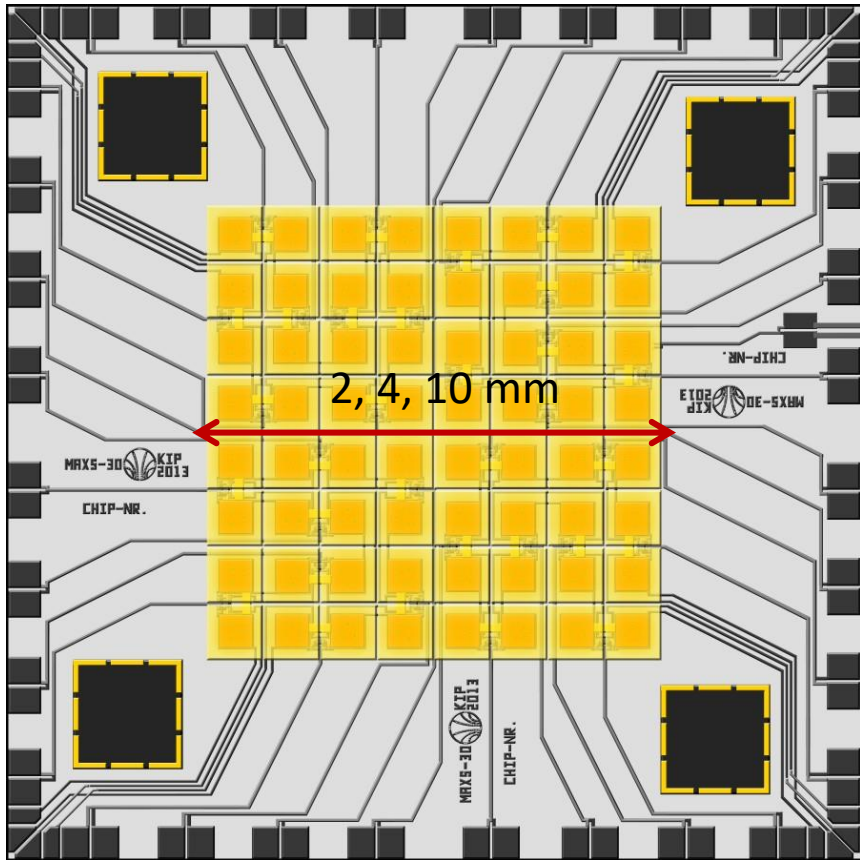
ECHO-100k wafer

Fabrication steps				
#	Layer	Material	Thickness	Deposition technique
1	Pick-up coils, SQUID lines (layer 1)	Nb	250 nm	Sputtering + etching
2	Isolation	Nb_2O_5	-	Anodisation
3	Isolation	SiO_2	175 nm	Sputtering + lift-off
4	Isolation	SiO_2	175 nm	Sputtering + lift-off
5	Heaters	AuPd	150 nm	Sputtering + lift-off
6	SQUID lines (layer 2)	Nb	600 nm	Sputtering + lift-off
7	Sensor	AgEr	480 nm	Sputtering + lift-off
8	Thermalisation	Au	300 nm	Sputtering + lift-off
9	Stems	Au	100 nm	Sputtering
10	Absorber - 1st layer	Au	3 μm	Electroplating + lift-off
11	^{163}Ho host material	Ag	100 nm	Sputtering
12	^{163}Ho implantation	^{163}Ho	-	Ion-implantation
13	^{163}Ho host material	Ag	100 nm	Sputtering + lift-off
14	Absorber - 2nd layer	Au	3 μm	Sputtering + lift-off





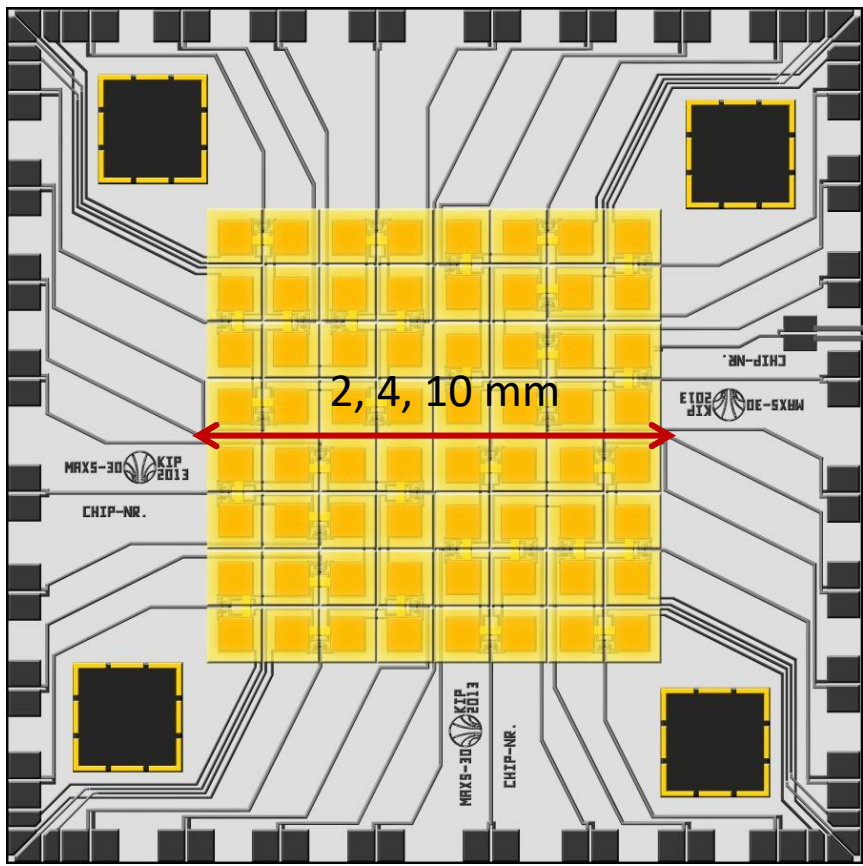
Microcalorimeter arrays for X-rays spectroscopy - maXs



maXs-20/30/100:

- 8x8 pixels for photons up to 20/30/100 keV
- with $\Delta E_{FWHM} = 2/5/30$ eV
- 32 two-stage dc-SQUIDS

Microcalorimeter arrays for X-rays spectroscopy - maXs

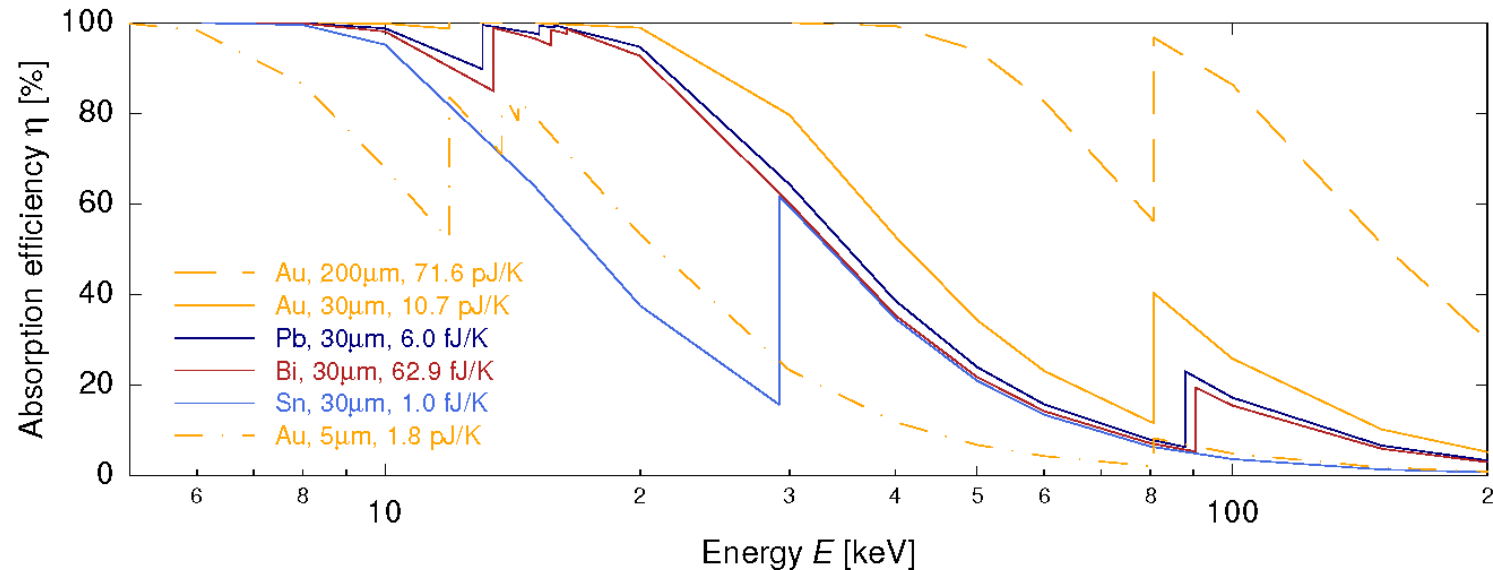


maXs-20/30/100:

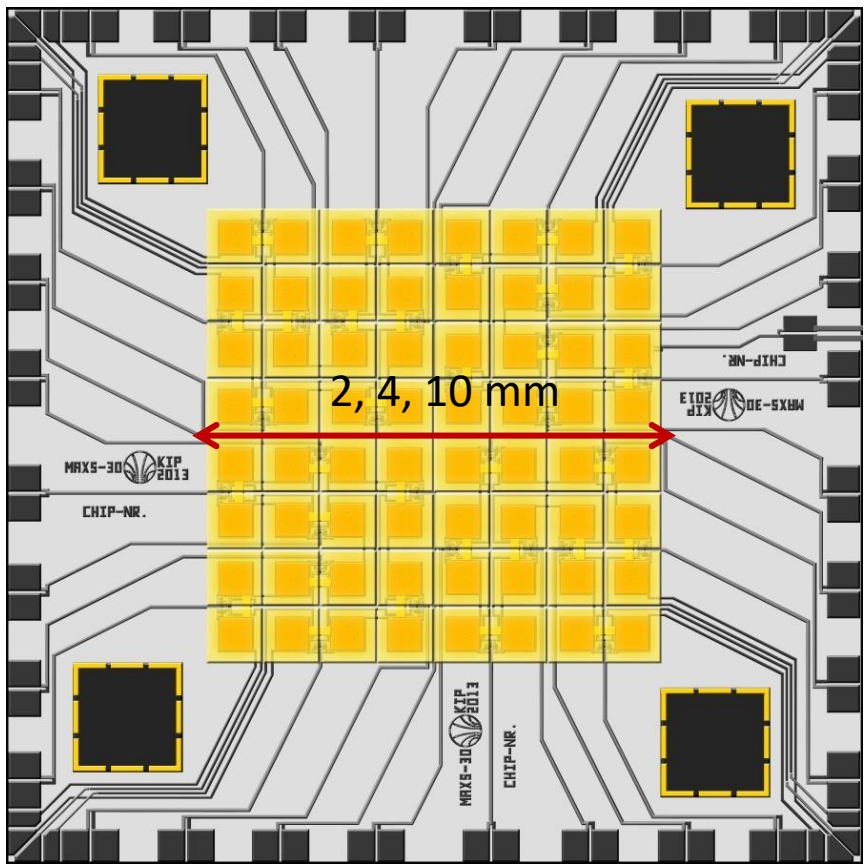
- 8x8 pixels for photons up to 20/30/100 keV
- with $\Delta E_{\text{FWHM}} = 2/5/30 \text{ eV}$
- **32 two-stage dc-SQUIDS**

Absorber material and thickness selected for optimal absorption efficiency

For maXs → **electroplated gold**

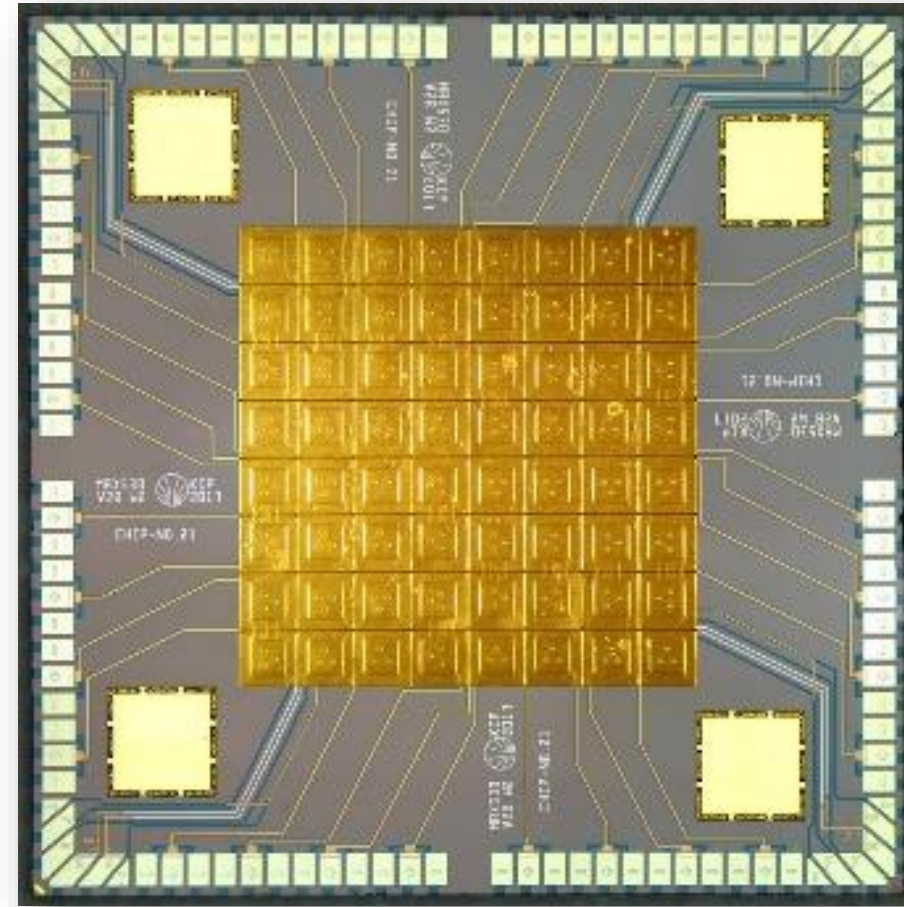


Microcalorimeter arrays for X-rays spectroscopy - maXs



maXs-20/30/100:

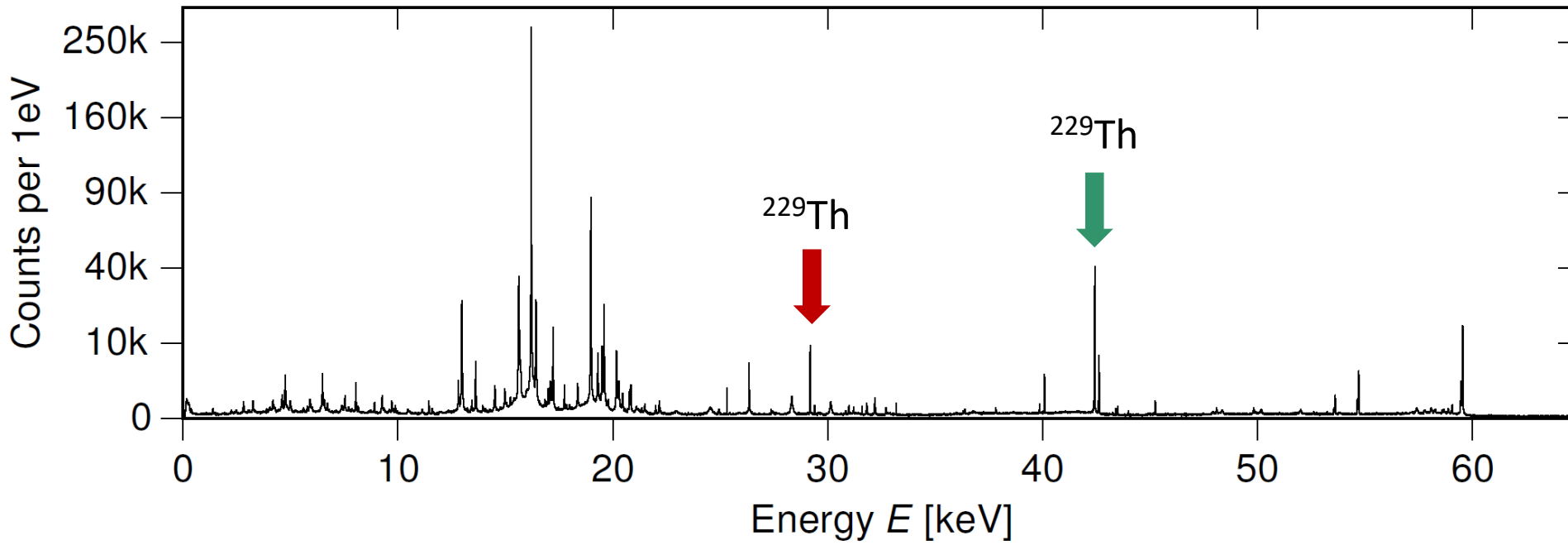
- 8×8 pixels for photons up to 20/30/100 keV
- with $\Delta E_{\text{FWHM}} = 2/5/30 \text{ eV}$
- 32 two-stage dc-SQUIDS



maXs-30

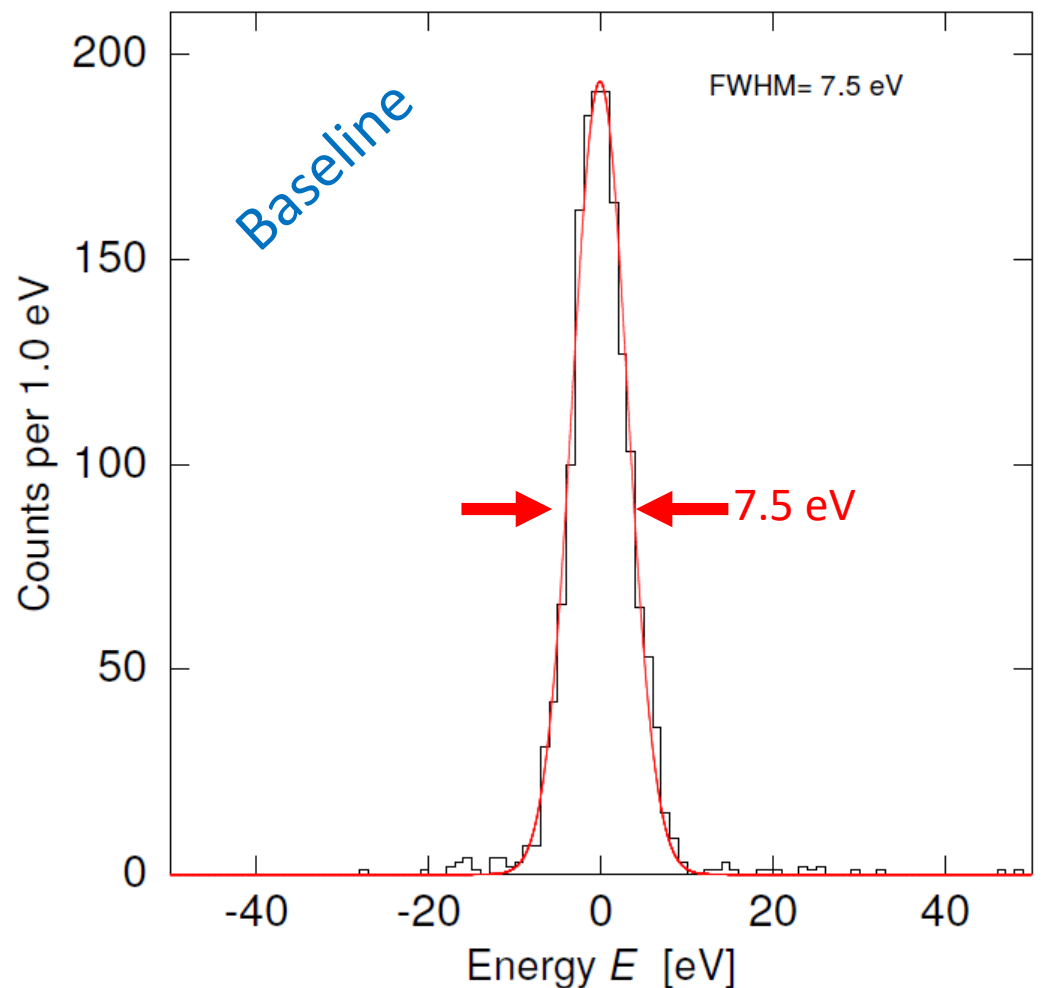
Absorber size: $500 \times 500 \times 30 \mu\text{m}^3$

maXs-30 with ^{241}Am + ^{233}U external sources

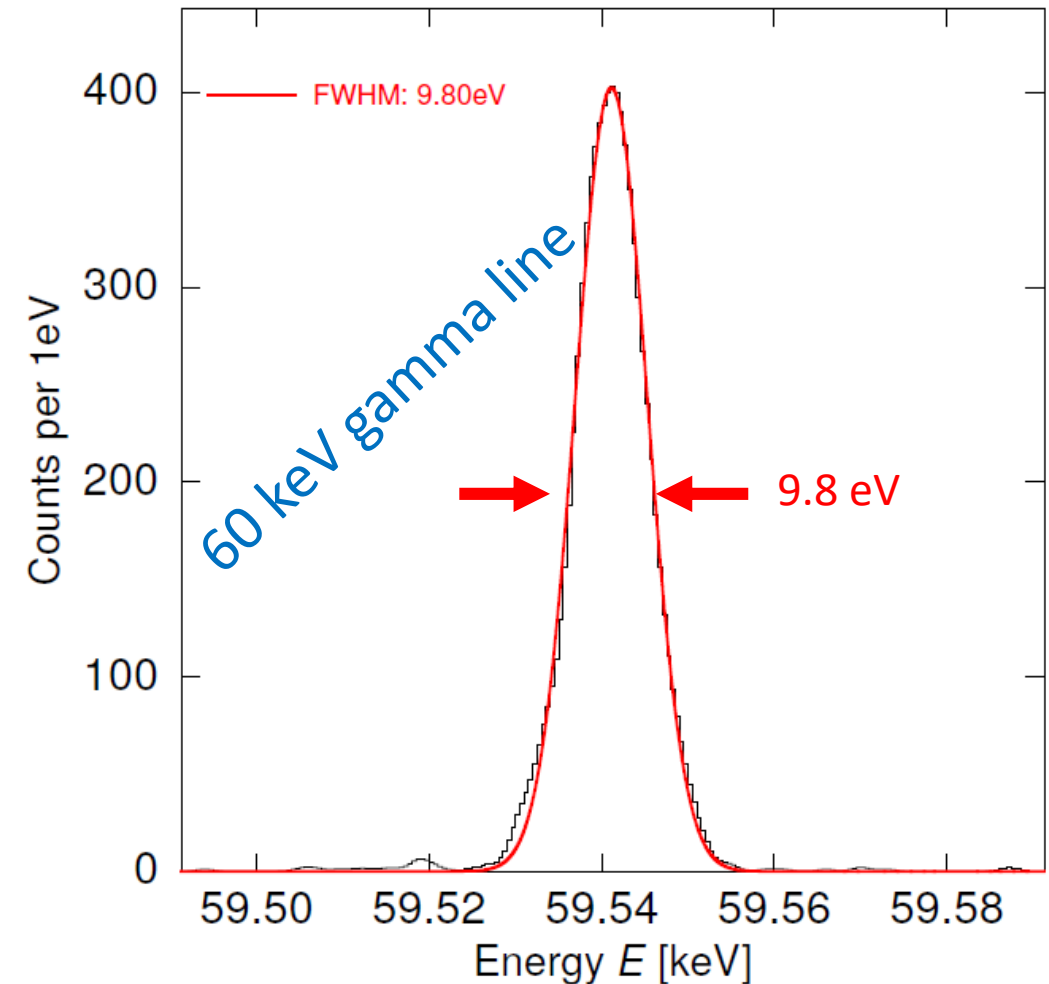


Co-added 20 channels, several weeks

maXs-30 with ^{241}Am + ^{233}U external sources



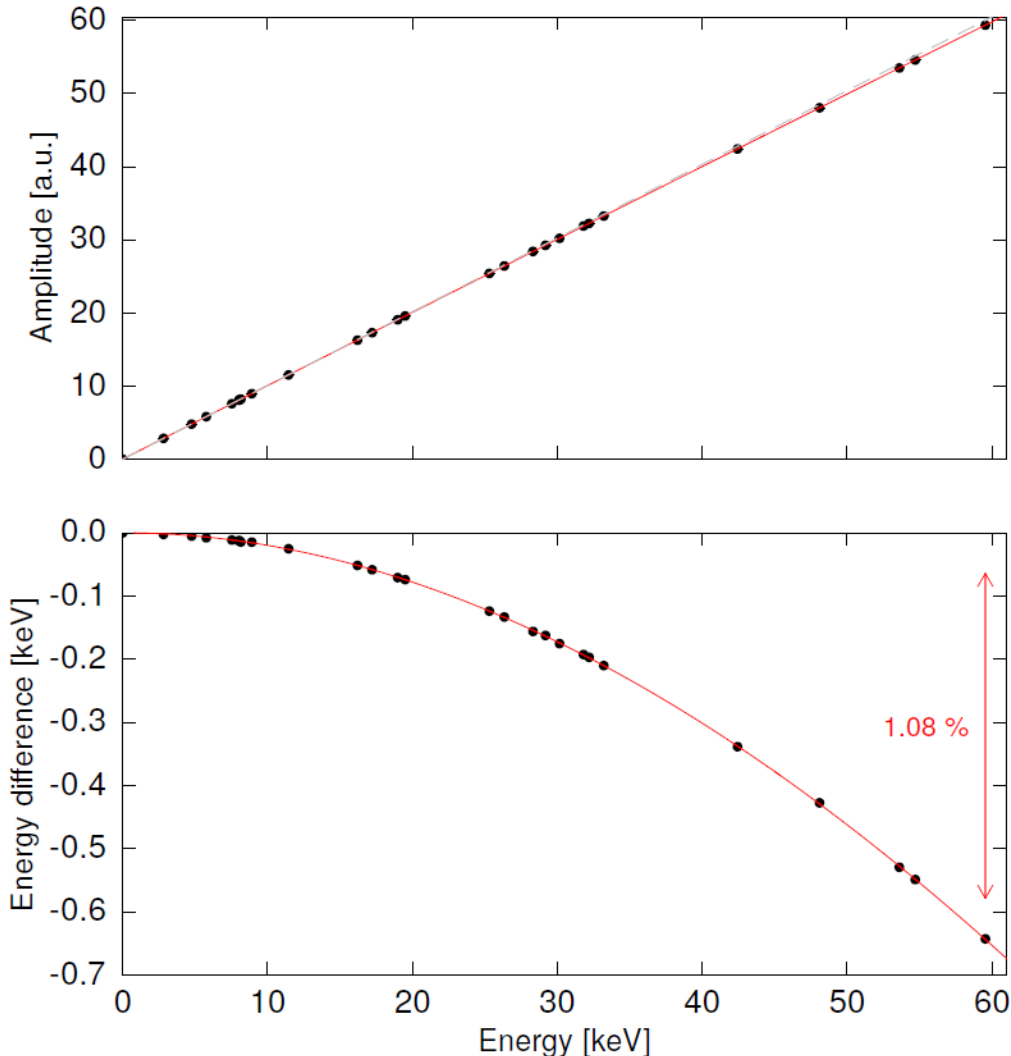
Very close to design value



Energy resolution $\Delta E_{\text{FWHM}} = 9.8 \text{ eV} @ 59 \text{ keV}$

World record resolving power: 6000

maXs-30 set-up - ^{241}Am + ^{233}U external sources

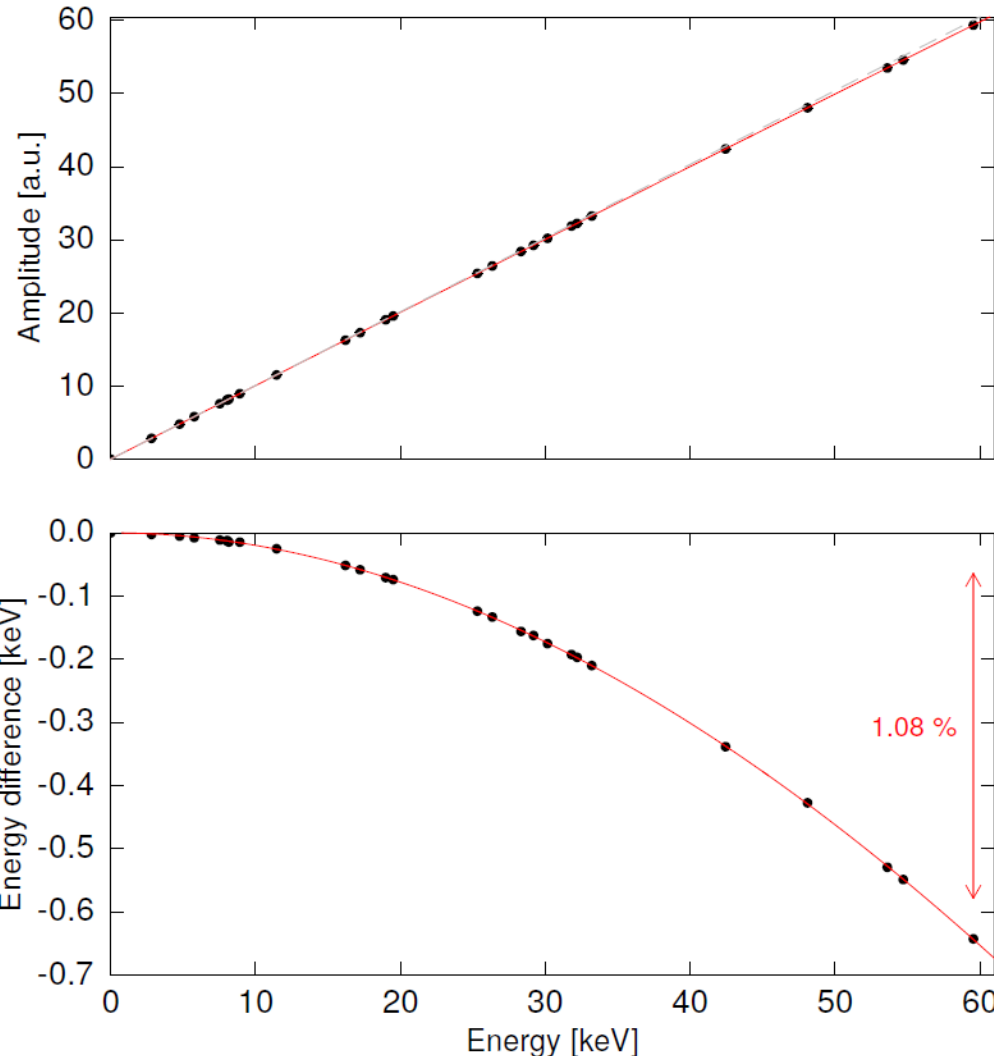


Energy calibration

- Polynomial function 2nd to 4th order
- Stable over long measuring time

non-linearity as expected from thermodynamics!

maXs-30 set-up - ^{241}Am + ^{233}U external sources

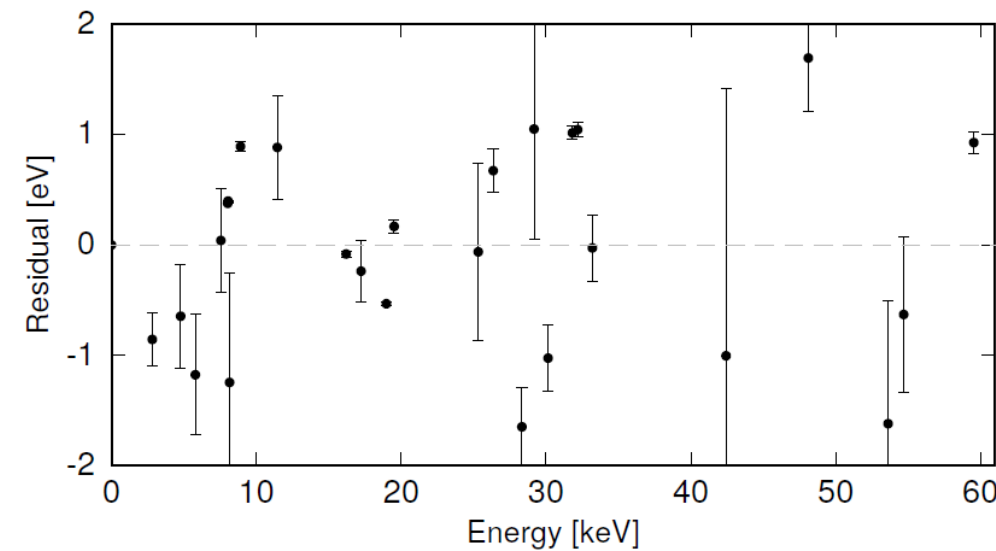


non-linearity as expected from thermodynamics!

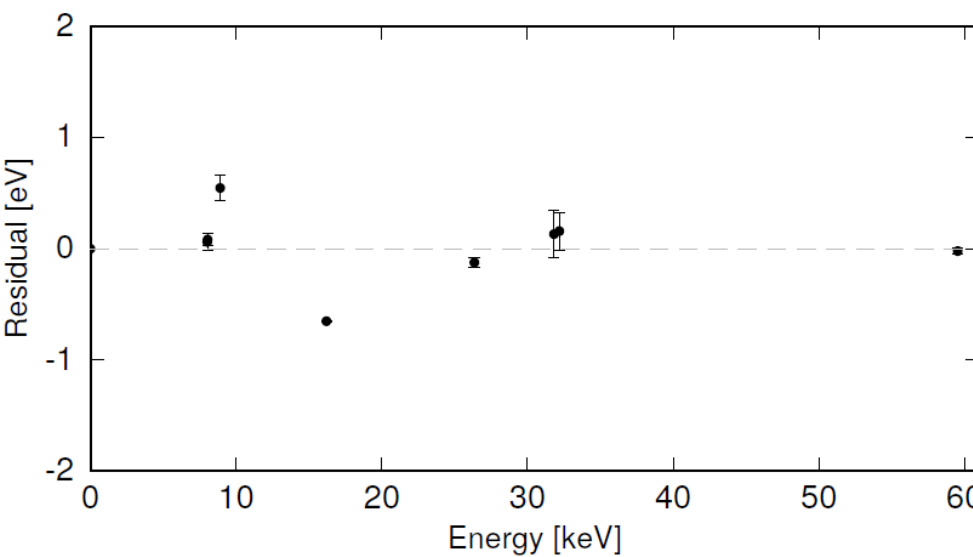
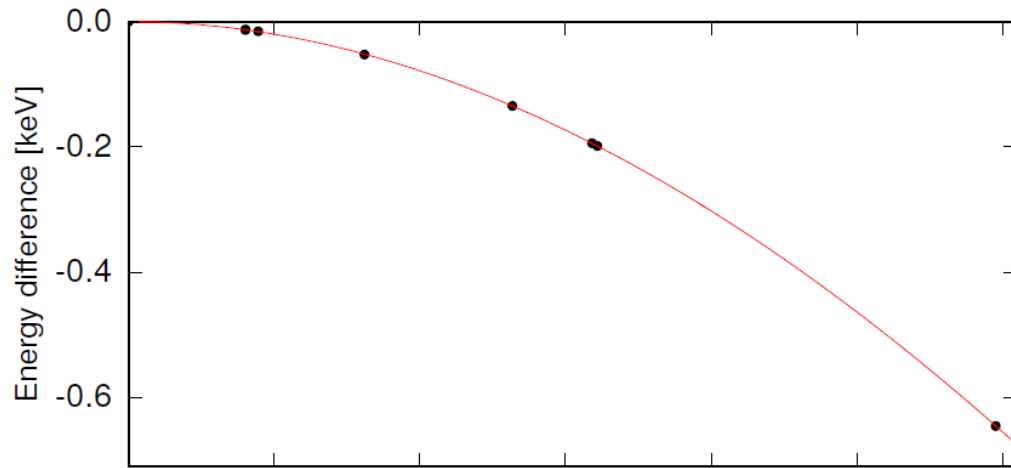
Energy calibration

- Polynomial function 2nd to 4th order
- Stable over long measuring time

Most lines from literature have too large uncertainty!



maXs-30 set-up - ^{241}Am + ^{233}U external sources

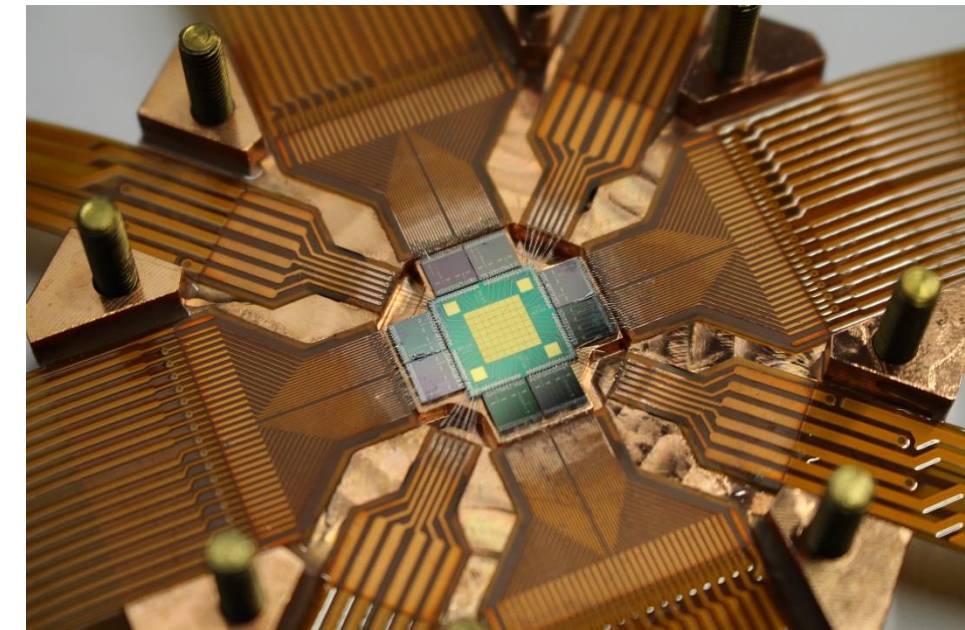


Energy calibration

- Polynomial function 2nd to 4th order
- Stable over long measuring time

Sub-eV agreement for carefully selected calibration lines.

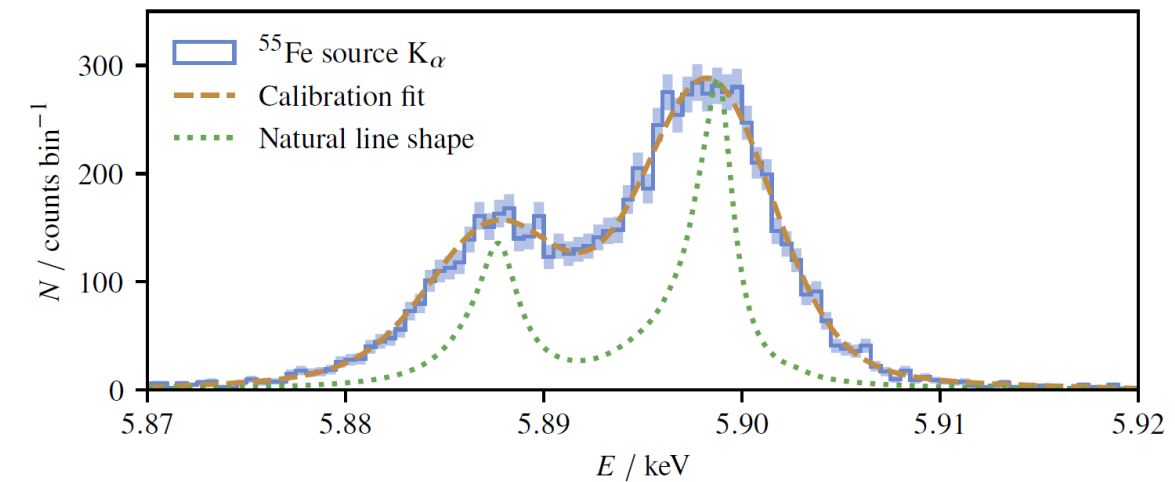
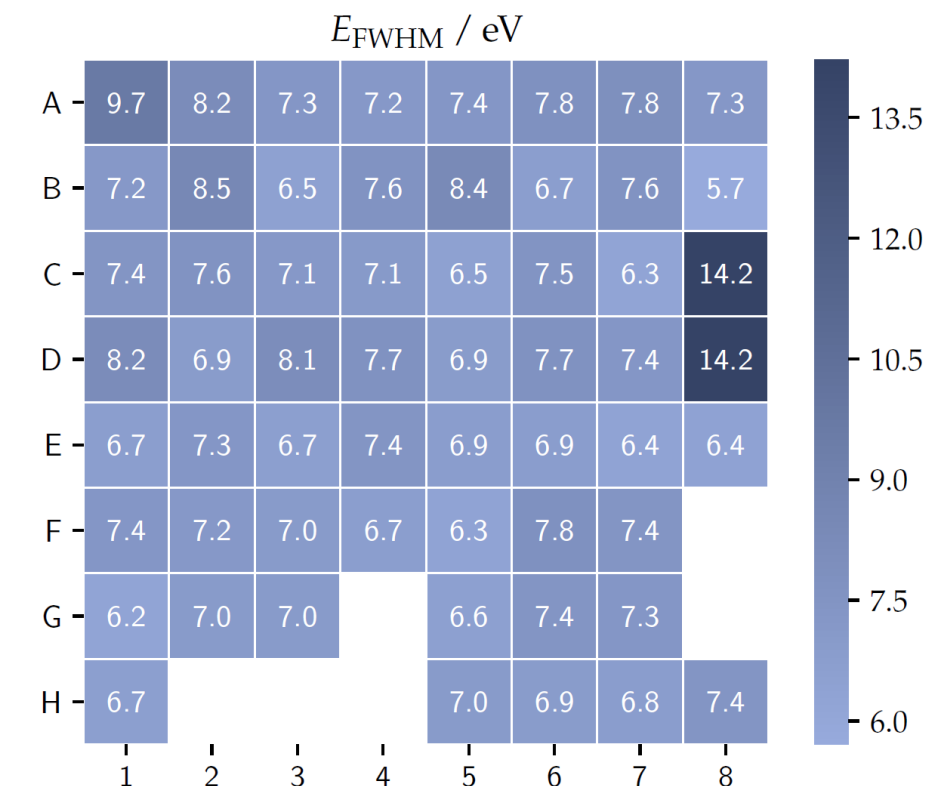
maXs-30 set-up – for IAXO



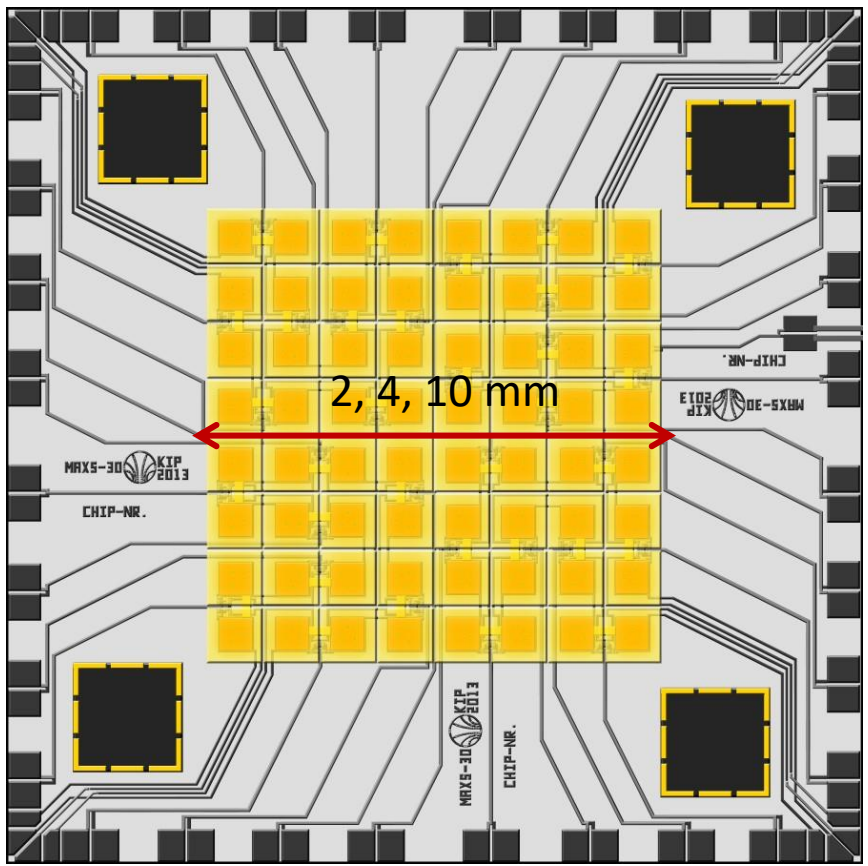
^{55}Fe calibration source
Stopping power @10 keV ~100%

- Homogeneous performance over the array
- Stable operation over 1 month

D. Unger et al., *JINST* **16** (2021) P06006,
[arXiv:2010.15348](https://arxiv.org/abs/2010.15348) [physics.ins-det]

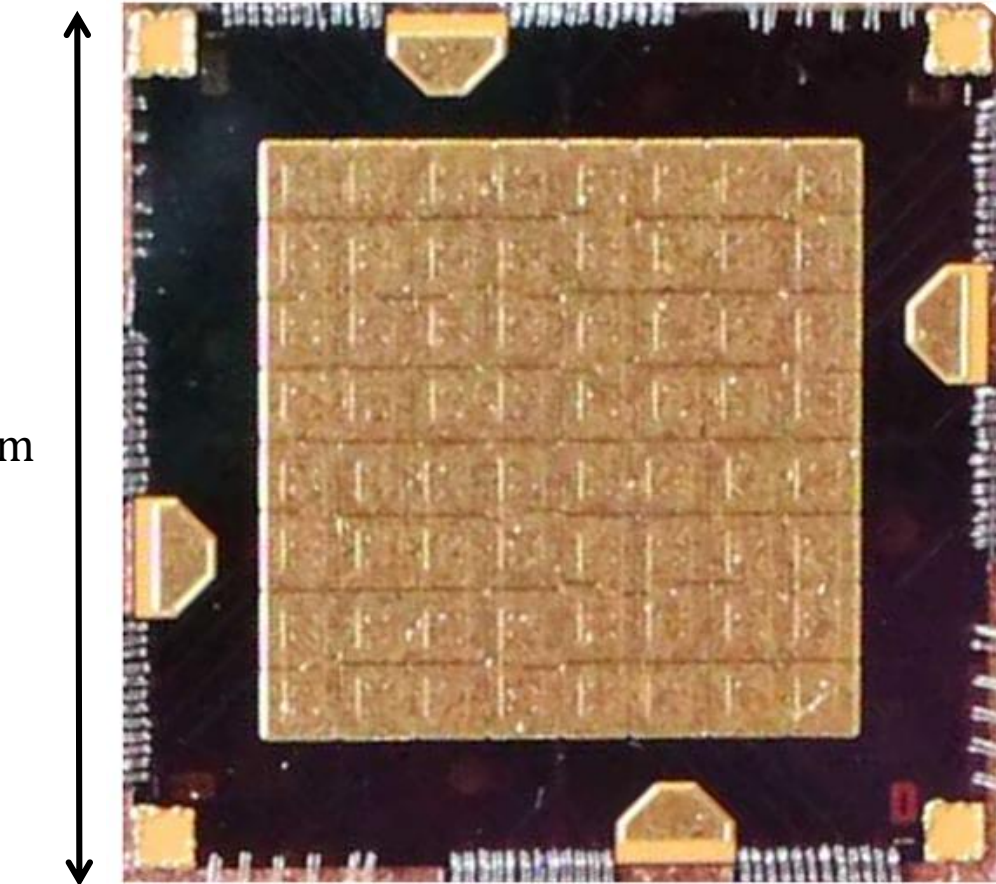


Microcalorimeter arrays for X-rays spectroscopy - maXs



maXs-20/30/100:

- 8x8 pixels for photons up to 20/30/100 keV
- with $\Delta E_{\text{FWHM}} = 2/5/30 \text{ eV}$
- **32 two-stage dc-SQUIDS**



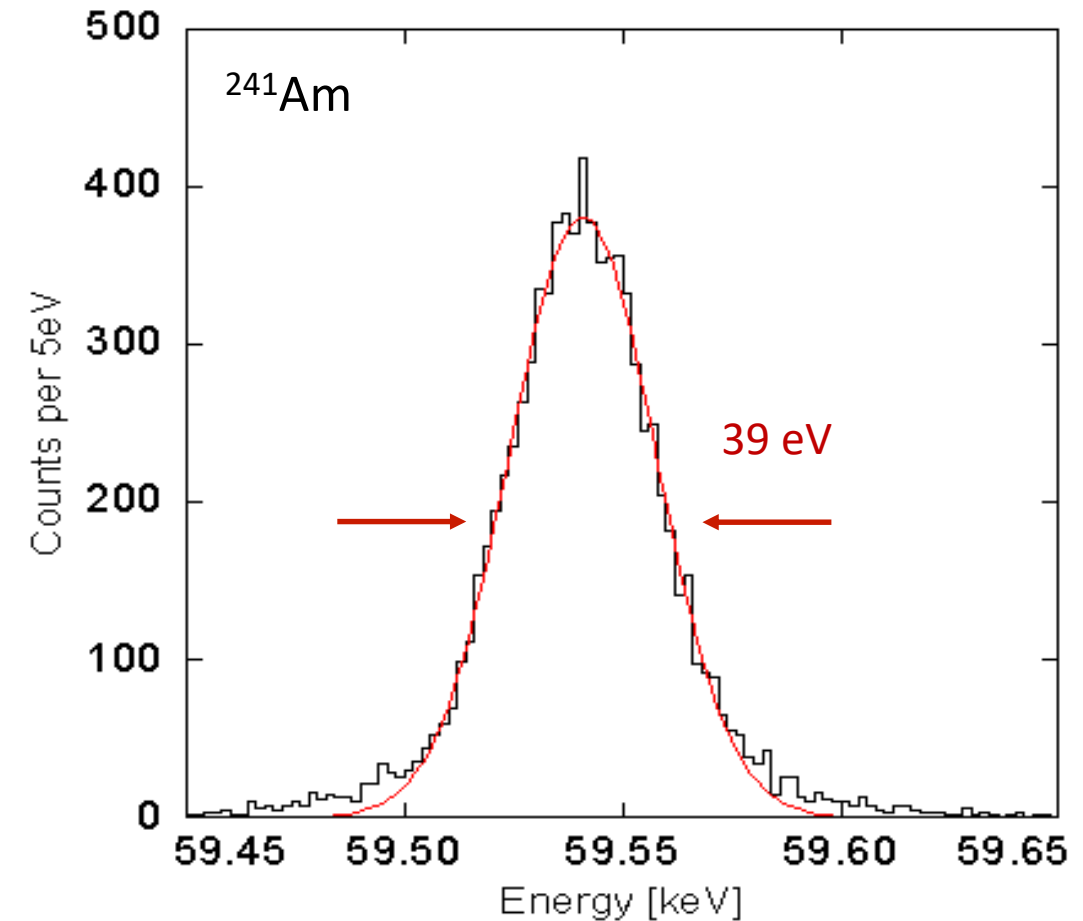
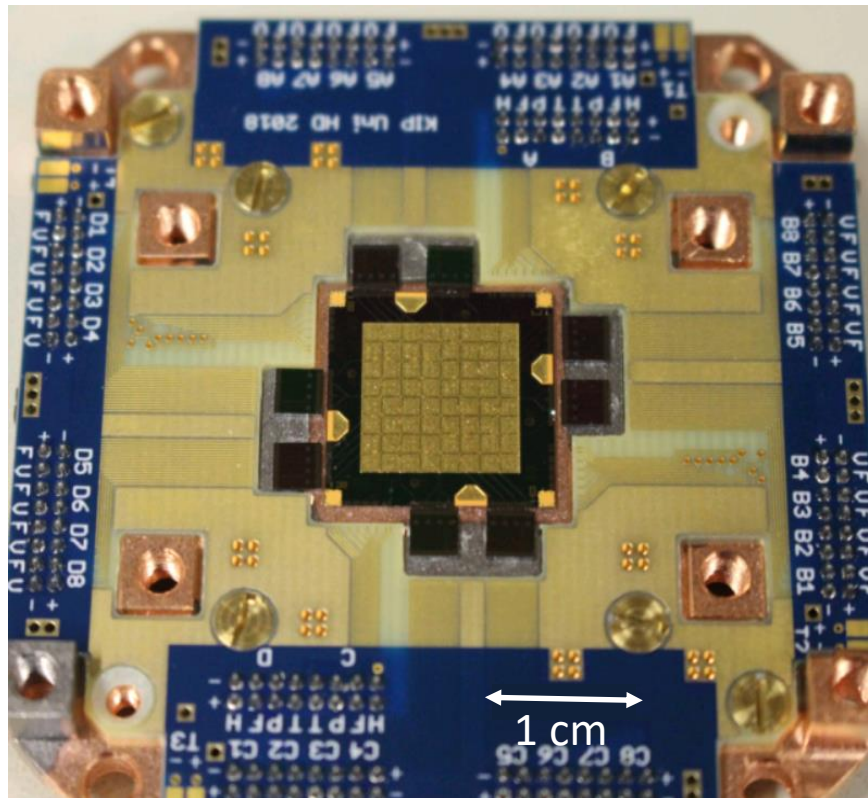
maXs-100

- Active area 8x8 absorbers
Area 1 cm^2
- **50 μm thick** electroplated gold
→ 40 % stopping power @ 100 keV

maXs-100 for highly ionized heavy ions

Study of **heavy, highly-charged** ions allows
high precision QED measurements in extreme E-fields
→ spectroscopy of H-like and He-like Uranium ions

Signal rise time limited to $\tau=8 \mu\text{s}$
→ Prevents position-dependent pulse shape
39 eV (FWHM) @ 60 keV (co-added spectrum from 30 pixels)



Experimental configuration @ GSI

Electron cooler

- Superimpose electron and ion beam
- Reduce momentum spread
- $U^{91+} + e^- \rightarrow U^{90+} + \gamma$

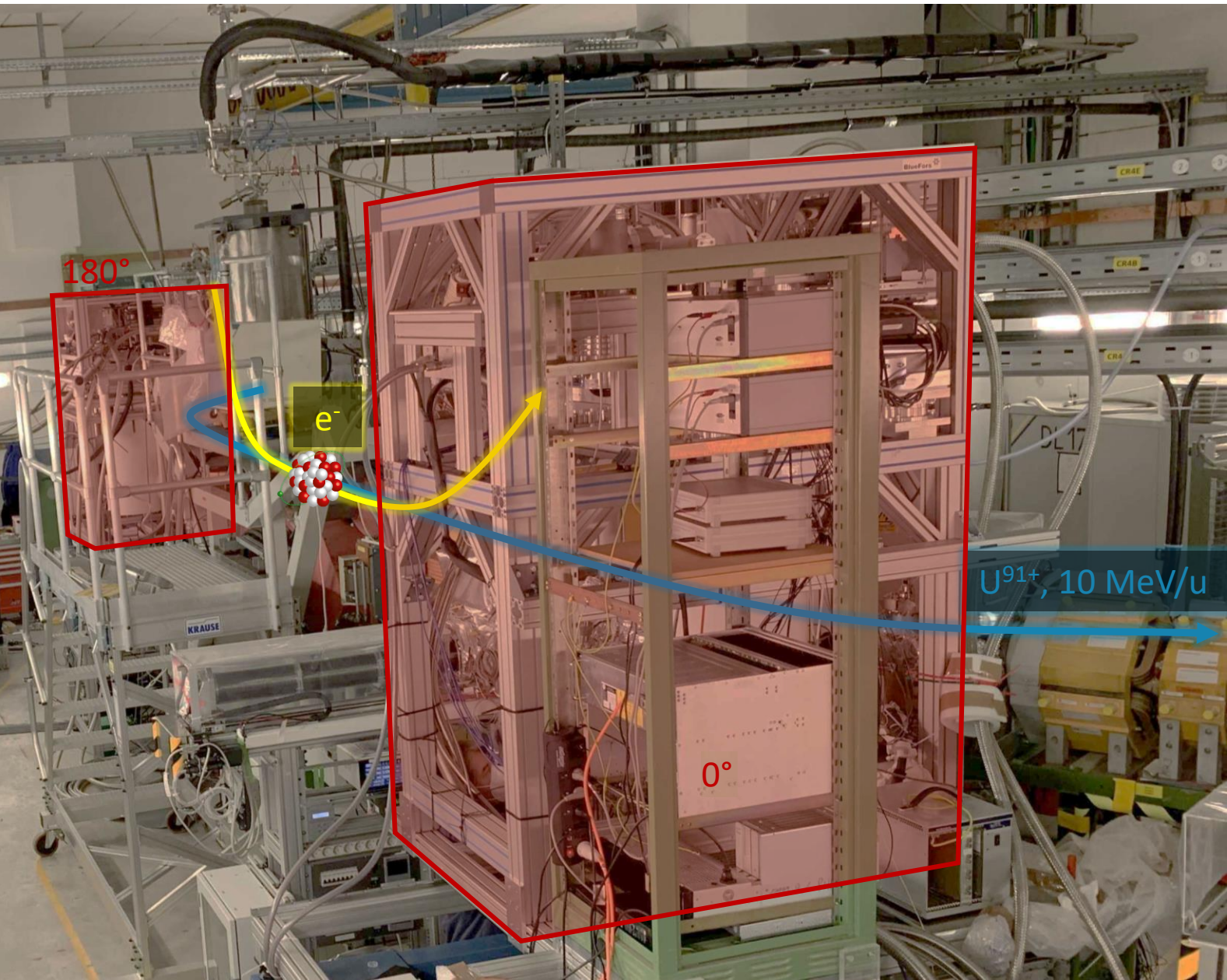
2 detector systems

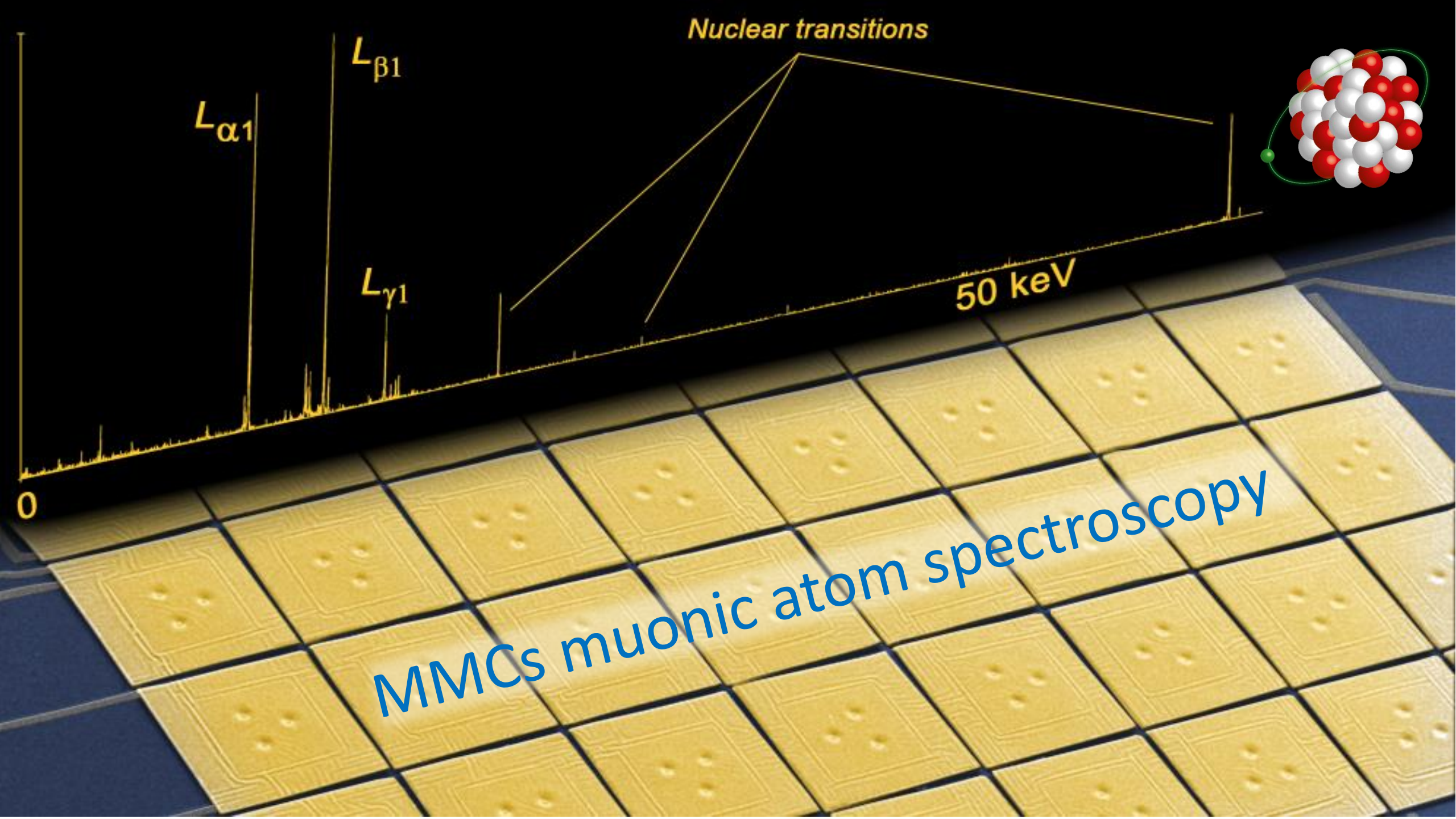
- At 0° and 180° scattering angle
- 13 keV red shift @ 180°
- 15 keV blue shift @ 0°
- intrinsic Doppler shift correction

2x maXs100

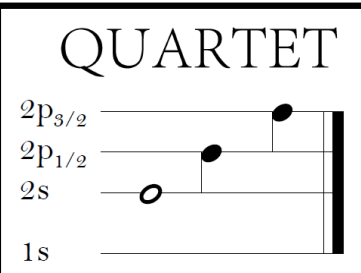
- In total 102/128 pixels operated
- Energy resolution
 - 80 eV FWHM @ 122 keV
 - 60 eV FWHM @ 122 keV

Composite calibration source





QUARTET*

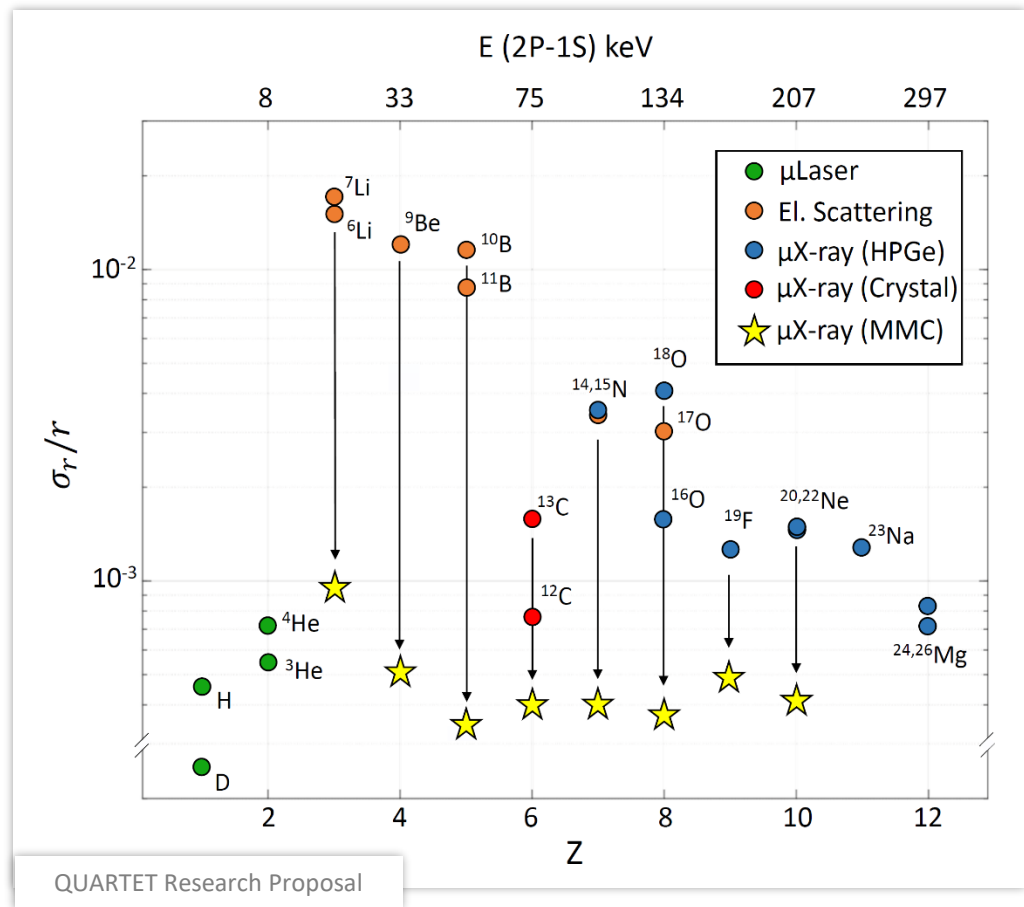
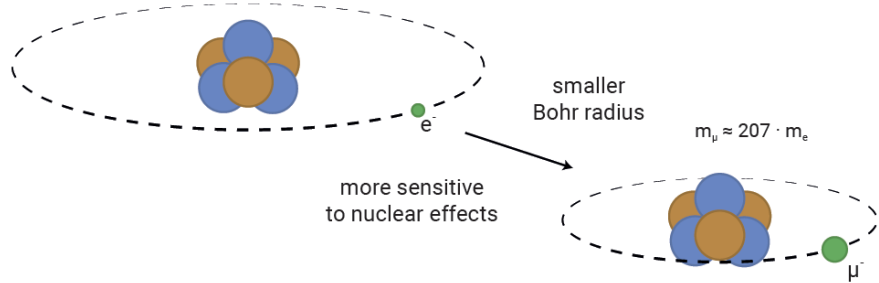


Precise measurement of absolute nuclear charge radii

- test of nuclear theory
- essential input parameter for QED tests
- search for physics beyond the Standard Model

Large accuracy gap for $2 < Z < 11$

- Improve precision of stable nuclei from ${}^6\text{Li}$ to ${}^{22}\text{Ne}$



QUARTET Collaboration

KU LEUVEN

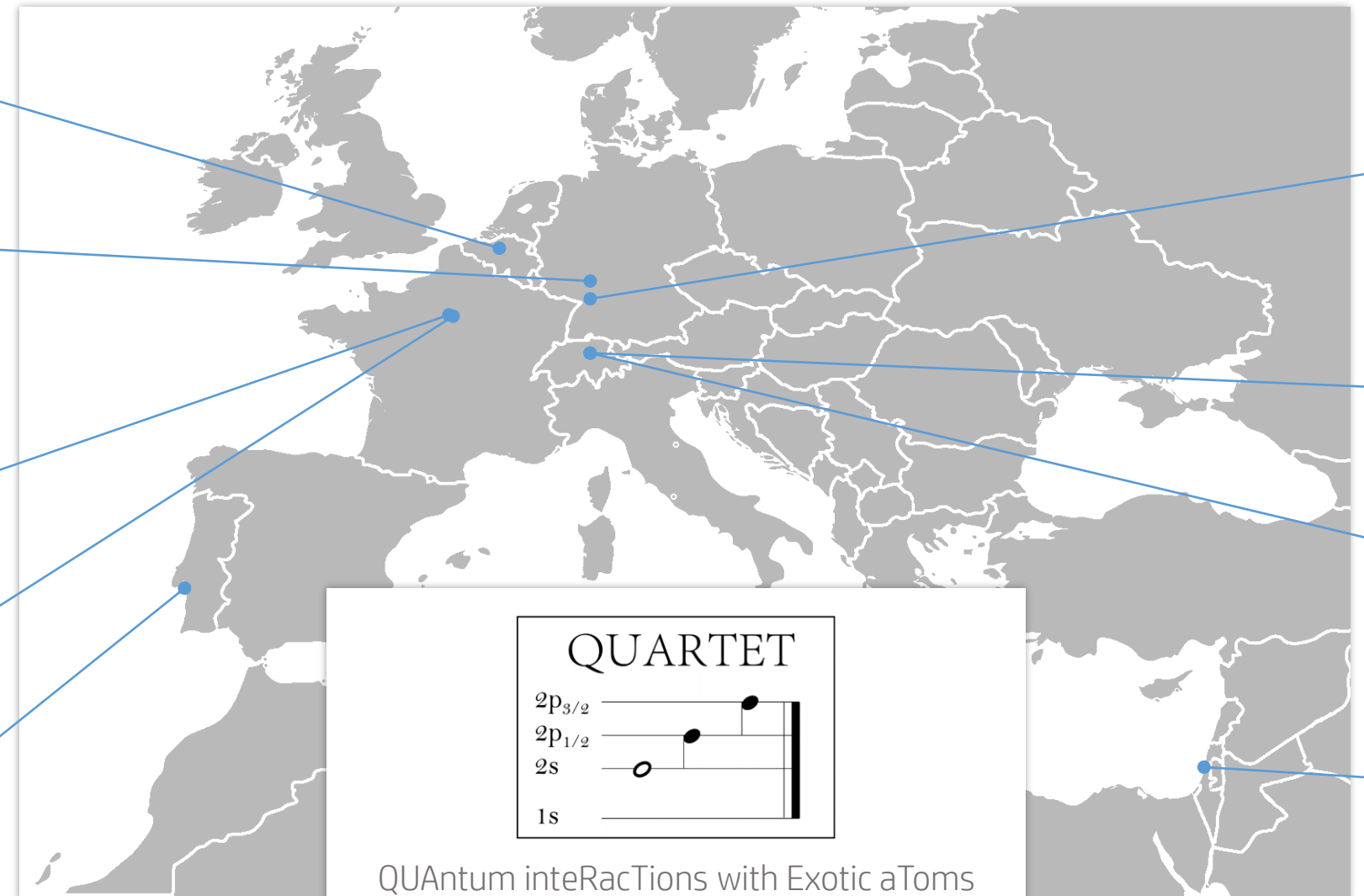


JOHANNES GUTENBERG
UNIVERSITÄT MAINZ

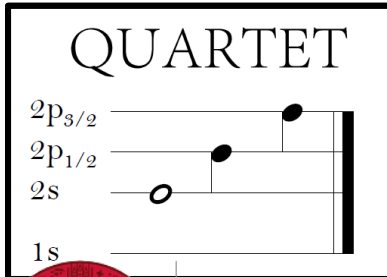
Laboratoire Kastler Brossel
Physique quantique et applications

université
PARIS-SACLAY

NOVA
UNIVERSIDADE NOVA
DE LISBOA



QUARTET
QUAntum inteRacTions with Exotic aToms
arXiv:2210.16929
Physics 2024, 6(1), 206-215
arXiv:2311.12014



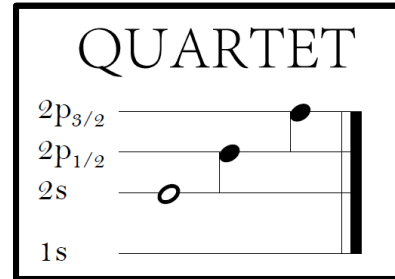
UNIVERSITÄT
HEIDELBERG
ZUKUNFT
SEIT 1386

PAUL SCHERRER INSTITUT
PSI

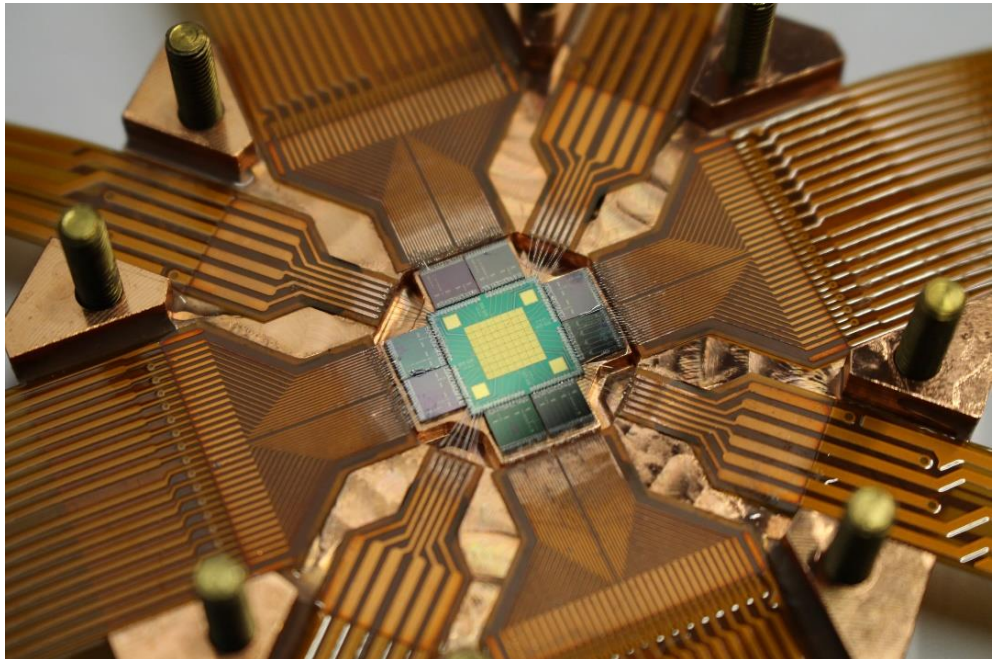
ETH zürich

 TECHNION
Israel Institute
of Technology

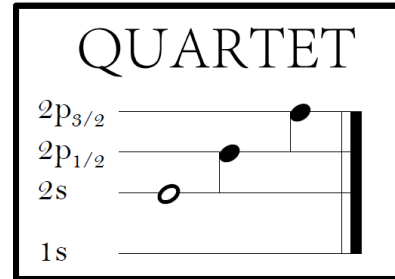
QUARTET – maXs-30



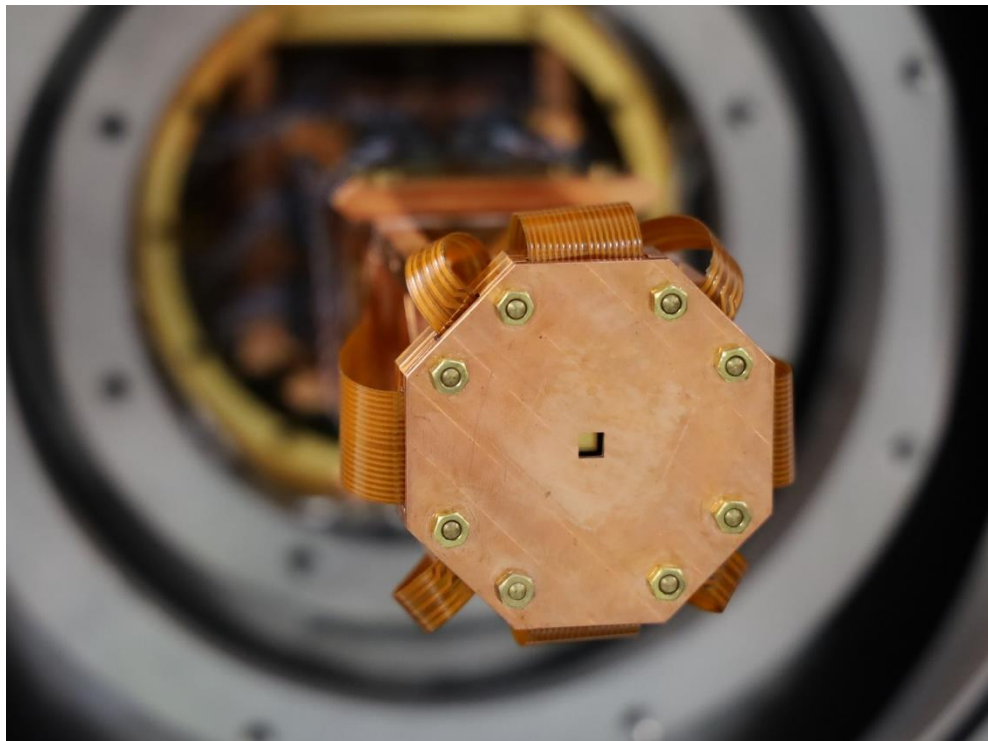
- Proof of concept experiment with muonic atoms
→ PSI measurements in October 2023
maXs-30 set-up



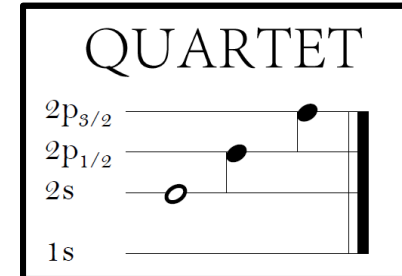
QUARTET – maXs-30



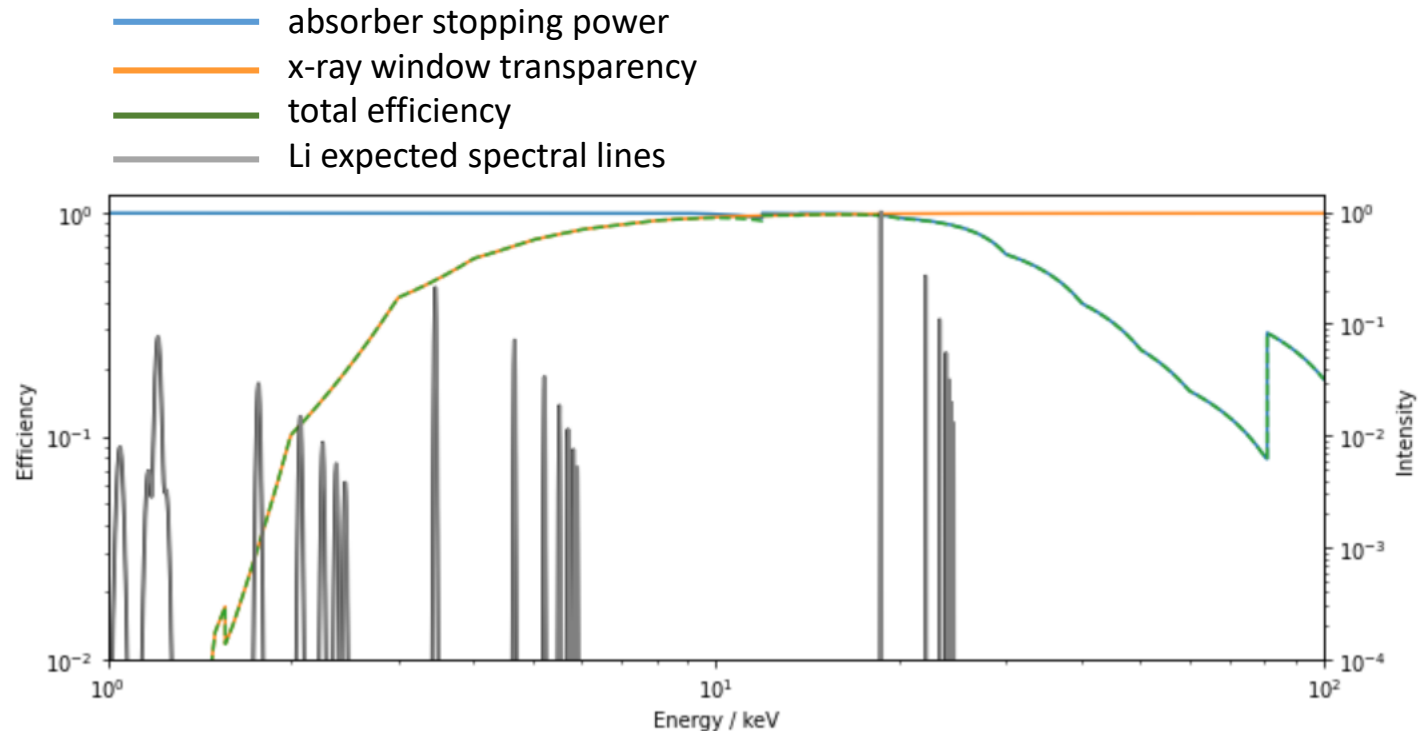
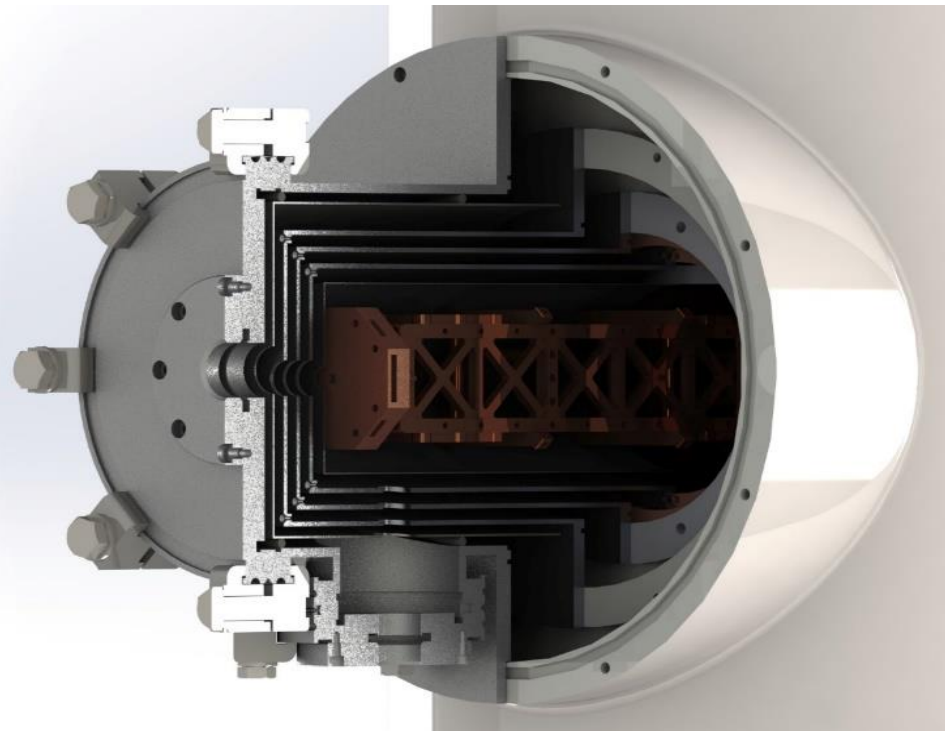
- Proof of concept experiment with muonic atoms
→ PSI measurements in October 2023
maXs-30 set-up on a side arm



QUARTET – maXs-30

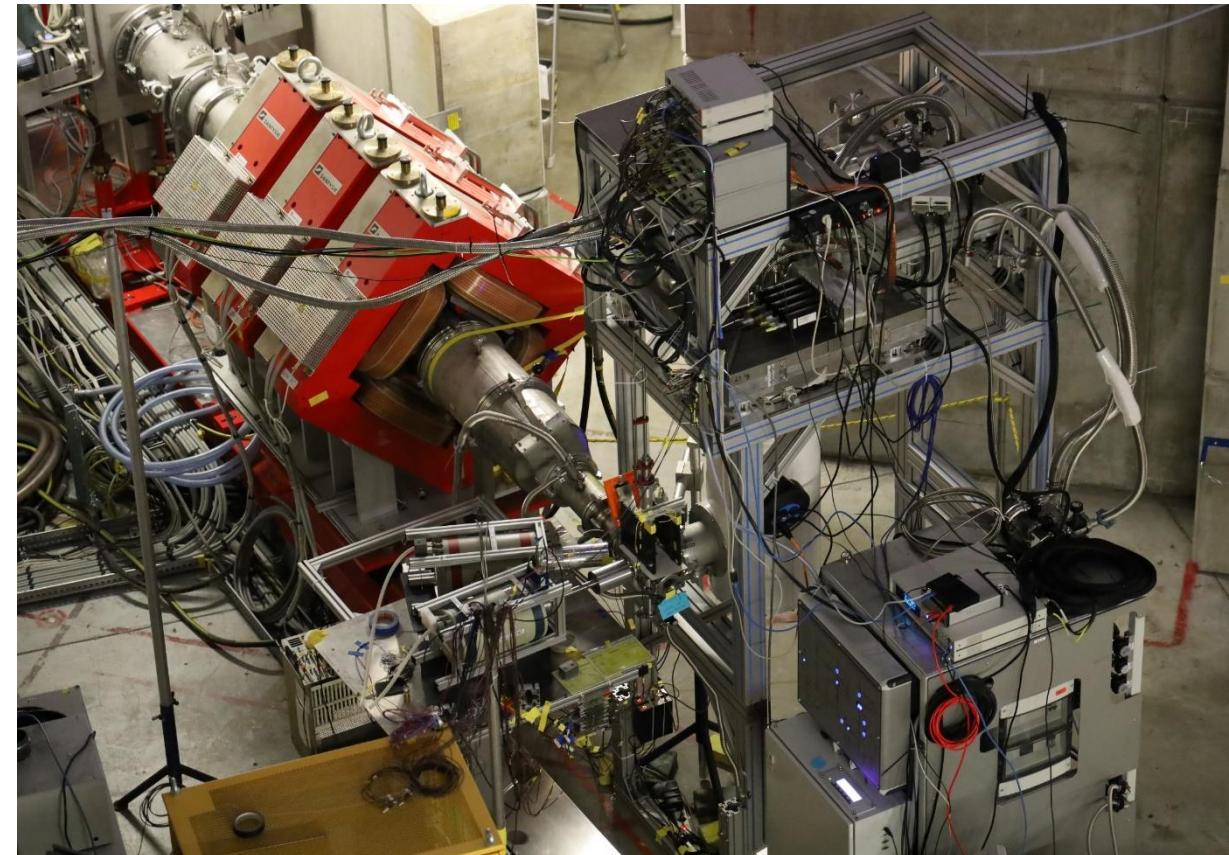
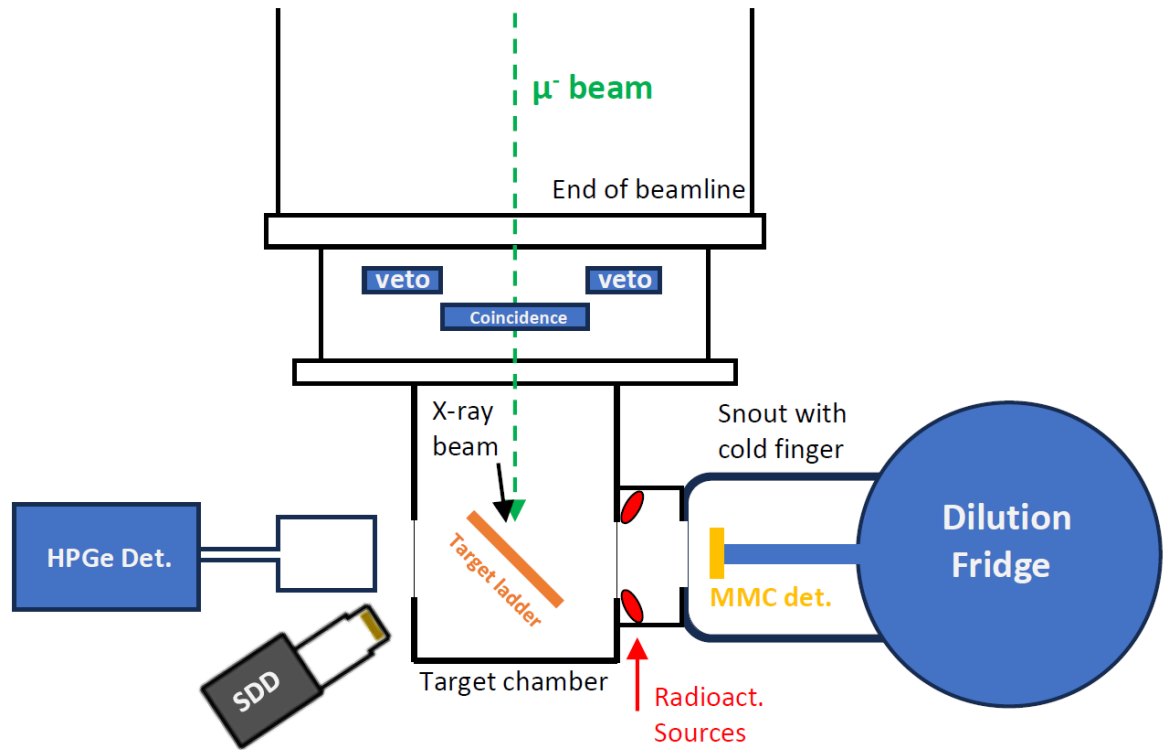
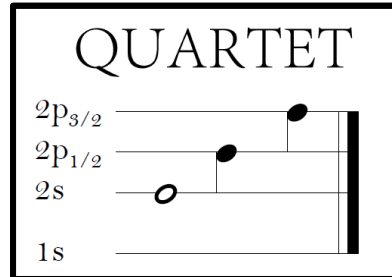


- Proof of concept experiment with muonic atoms
→ PSI measurements in October 2023
maXs-30 set-up on a side arm with x-ray windows

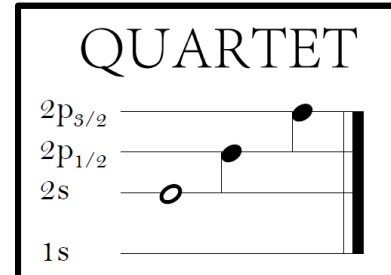


QUARTET – Beamtime 2023

Cryogenic system integrated with existing muon, electron and photon detector

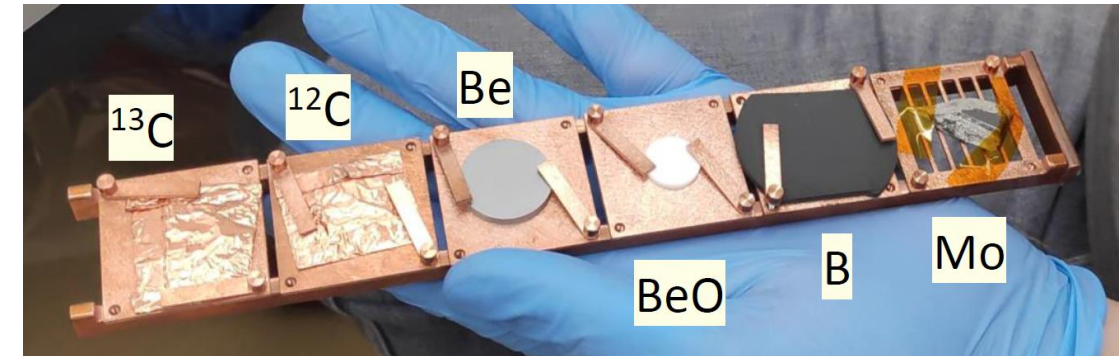
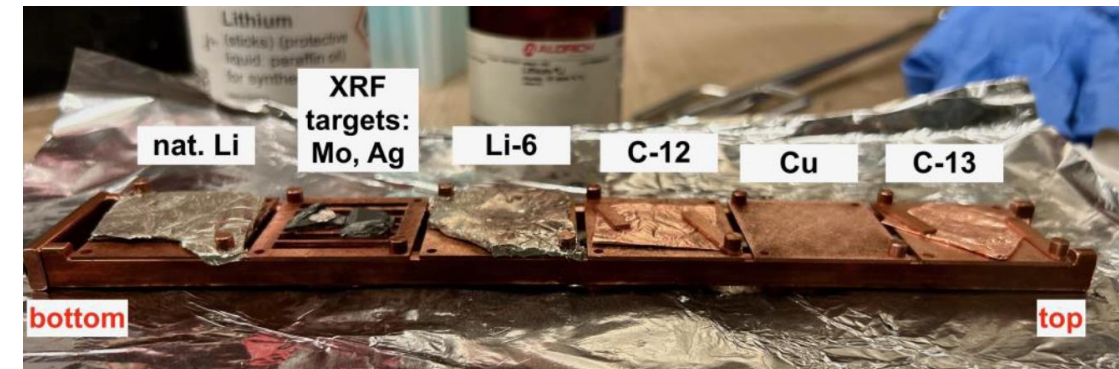
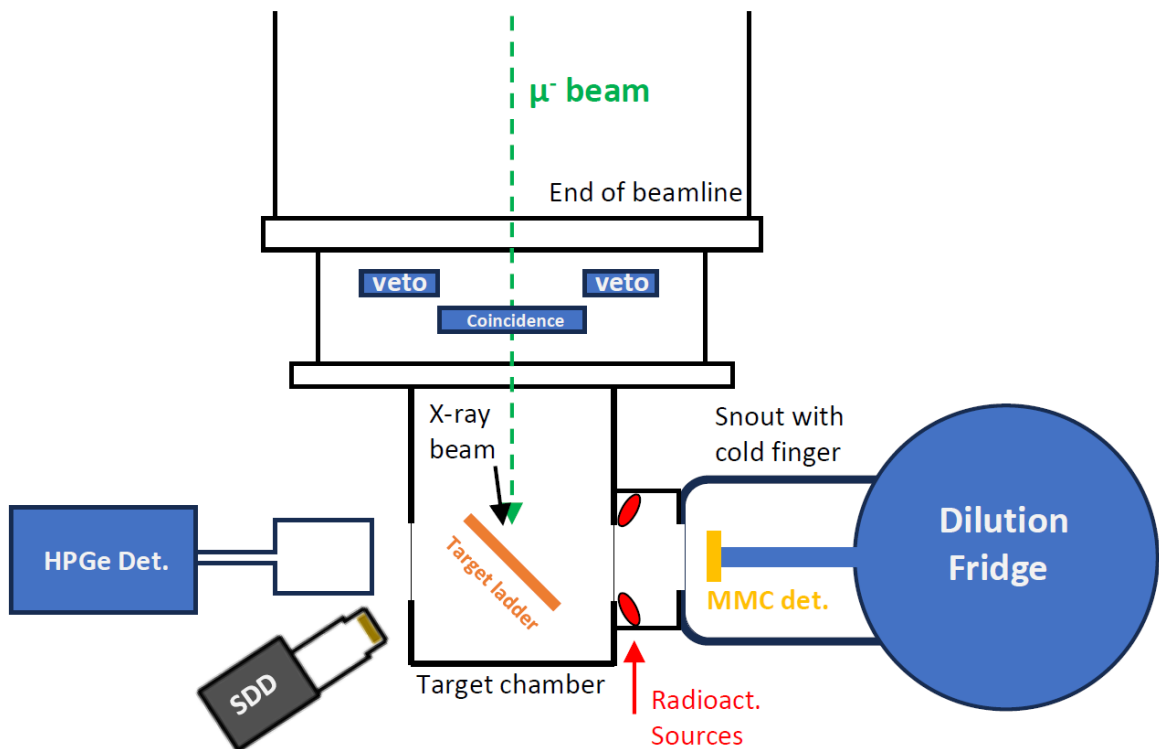


QUARTET – Beamtime 2023

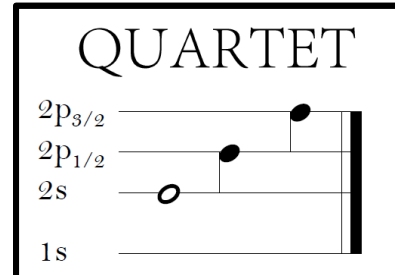


Cryogenic system integrated with existing muon, electron and photon detector

- Target:**
- Natural abundance (95% ^7Li) pure lithium metal foil
 - Enriched 95% ^6Li lithium metal foil
 - ^9Be cylinder and ^9BeO cylinder
 - Natural abundance (80% ^{11}B , 20% ^{10}B) boron foil
 - Enriched ^{12}C powder
 - Enriched ^{13}C D-fructose powder



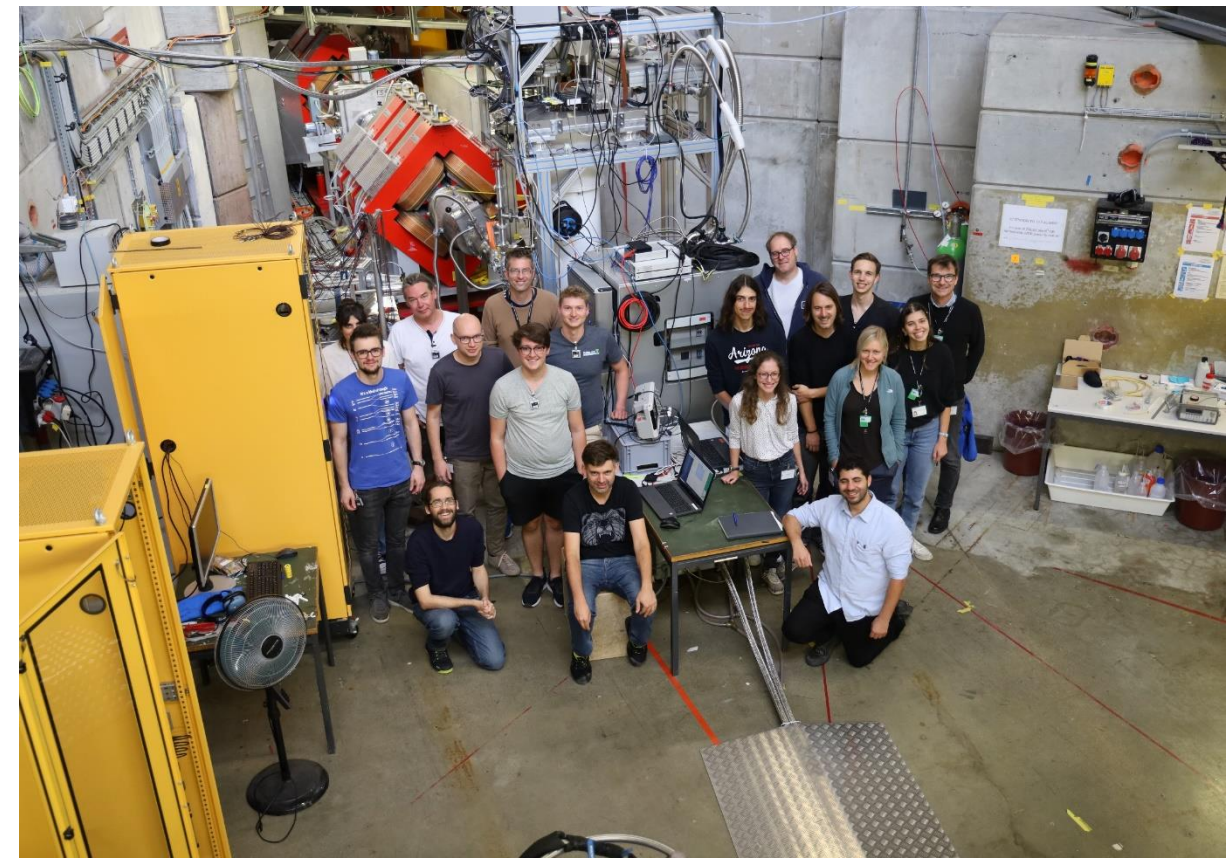
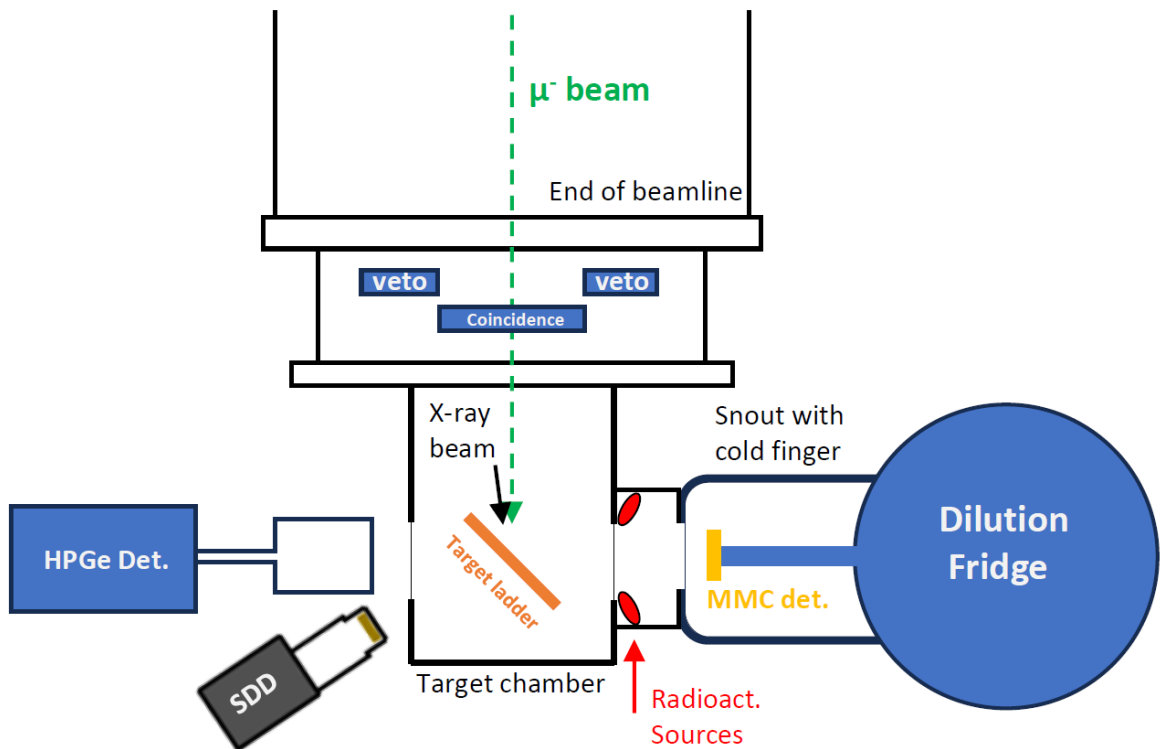
QUARTET – Beamtime 2023



Cryogenic system integrated with existing muon, electron and photon detector

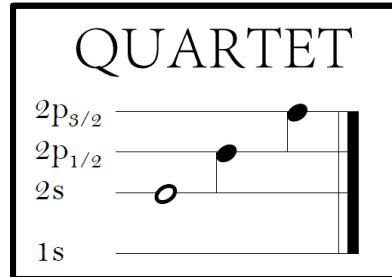
Target:

- Natural abundance (95% ⁷Li) pure lithium metal foil
- Enriched 95% ⁶Li lithium metal foil
- ⁹Be cylinder and ⁹BeO cylinder
- Natural abundance (80% ¹¹B, 20% ¹⁰B) boron foil
- Enriched ¹²C powder
- Enriched ¹³C D-fructose powder



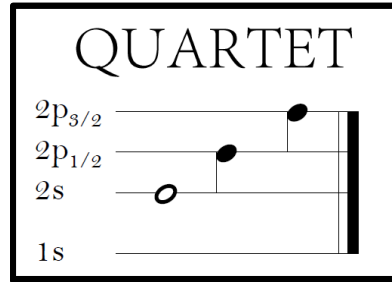
QUARTET – Preliminary results

- Detector operation > 95% of the time
- Excellent energy resolution
- Good rate for high precision line determination for Li, Be, B
- Rate for C should be increased → target optimization
→ single pixel optimization



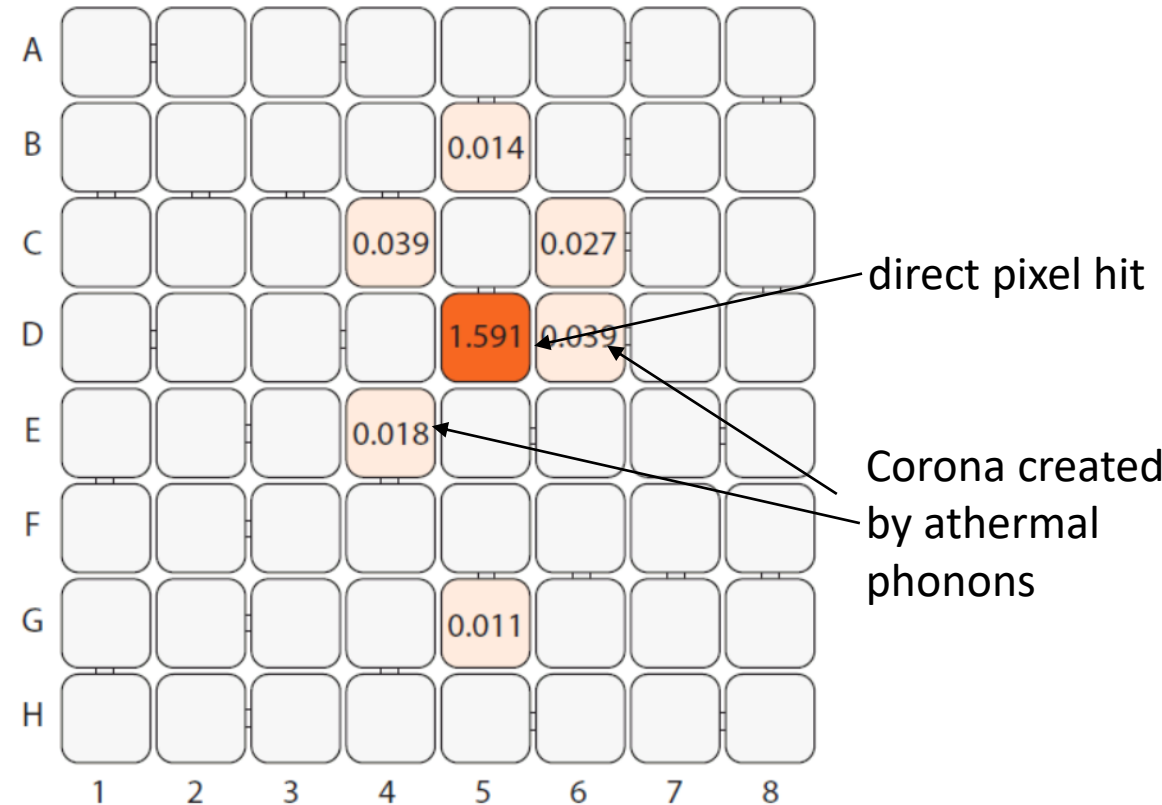
Target	E_{2P-1S} keV	ΔE_{FWHM} eV	Rate Hz	Expected Hz	BGD Hz keV $^{-1}$	Calib. source
Base	0	12				
⁶ Li	19	14	0.17	0.17	0.003	Mo K_α
⁷ Li	19	15	0.16	0.17	0.002	Mo K_α
⁹ Be	33	24	0.11	0.11	0.005	¹³⁷ Cs → Ba K_α
^{10,11} B	52	29	0.036	0.040	0.003	²⁴¹ Am
¹² C	75	~ 40	0.005	0.006	0.002	

QUARTET – Preliminary results



- Detector operation > 95% of the time
- Excellent energy resolution
- Good rate for high precision line determination for Li, Be, B
- Rate for C should be increased
 - target optimization
 - single pixel optimization
- Background suppression via coincidence with muons and Michel electrons

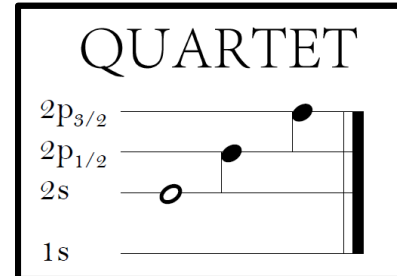
Target	E_{2P-1S} keV	ΔE_{FWHM} eV	Rate Hz	Expected Hz	BGD Hz keV $^{-1}$	Calib. source
Base	0	12				
⁶ Li	19	14	0.17	0.17	0.003	Mo K_α
⁷ Li	19	15	0.16	0.17	0.002	Mo K_α
⁹ Be	33	24	0.11	0.11	0.005	¹³⁷ Cs \rightarrow Ba K_α
^{10,11} B	52	29	0.036	0.040	0.003	²⁴¹ Am
¹² C	75	~ 40	0.005	0.006	0.002	



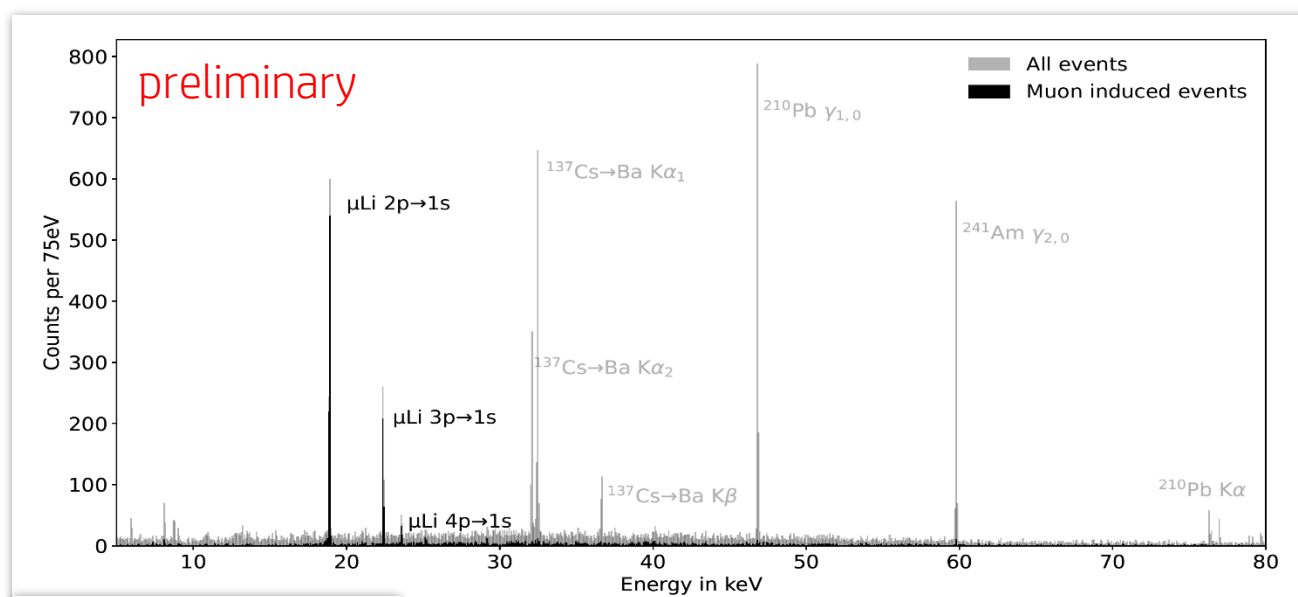
- Resulting from muon decay
- Deposit ~ 150 keV energy in the Si substrate
- Identified by signal shape and clustering

QUARTET – Preliminary results

- Detector operation > 95% of the time
- Excellent energy resolution
- Good rate for high precision line determination for Li, Be, B
- Rate for C should be increased → target optimization
→ single pixel optimization
- Background suppression via coincidence with muons and Michel electrons
- Excellent preliminary results
 - Muon coincidence allows for effective background suppression
 - $\mu\text{Li np} \rightarrow 1\text{s}$ transitions detected

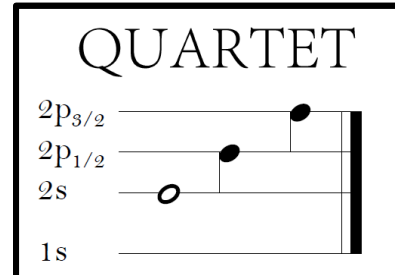


Target	$E_{2\text{p}-1\text{s}}$ keV	ΔE_{FWHM} eV	Rate Hz	Expected Hz	BGD Hz keV $^{-1}$	Calib. source
Base	0	12				
⁶ Li	19	14	0.17	0.17	0.003	Mo K_α
⁷ Li	19	15	0.16	0.17	0.002	Mo K_α
⁹ Be	33	24	0.11	0.11	0.005	¹³⁷ Cs \rightarrow Ba K_α
^{10,11} B	52	29	0.036	0.040	0.003	²⁴¹ Am
¹² C	75	~ 40	0.005	0.006	0.002	

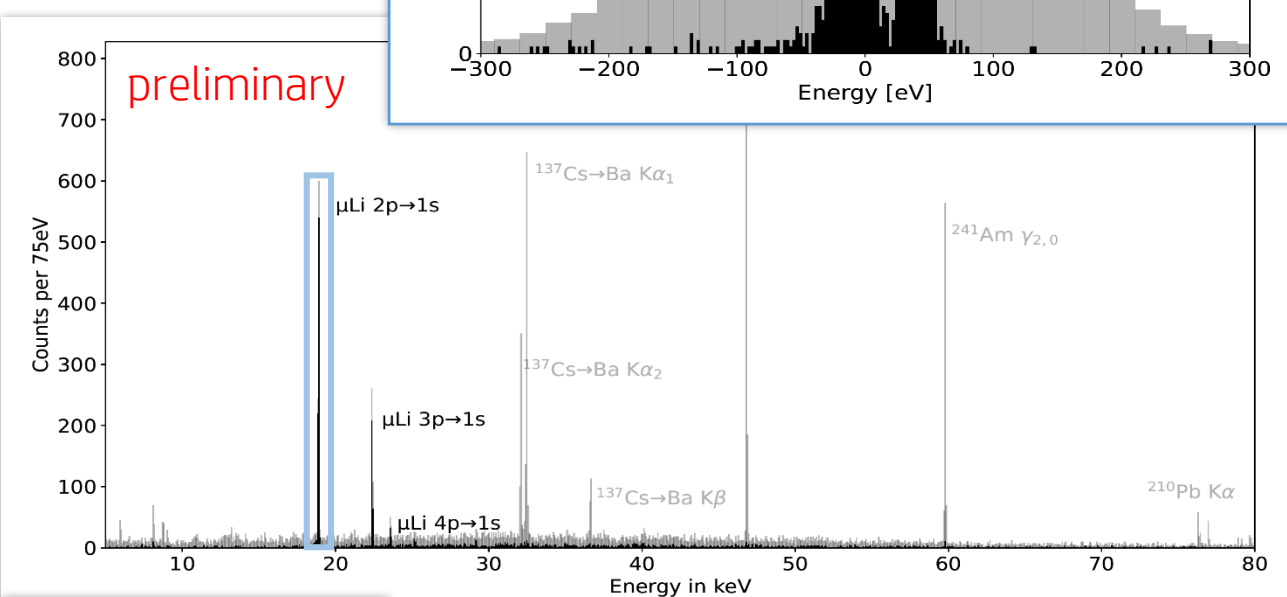
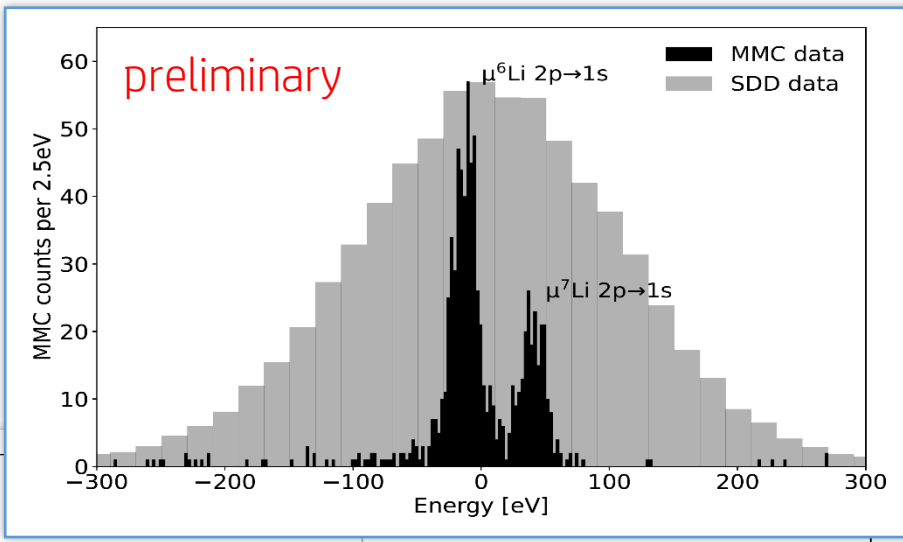


QUARTET – Preliminary results

- Detector operation > 95% of the time
- Excellent energy resolution
- Good rate for high precision line determination for Li, Be, B
- Rate for C should be increased → target optimization
→ single pixel optimization
- Background suppression via coincidence with muons and Michel electrons
- Excellent preliminary results
 - Muon coincidence allows for effective background suppression
 - $\mu\text{Li np} \rightarrow 1\text{s}$ transitions detected



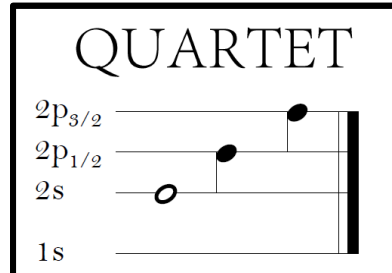
Isotope shift of muonic
 ^6Li and ^7Li resolved !



Target	$E_{2\text{p}-1\text{s}}$ keV	ΔE_{FWHM} eV	Rate Hz	Expected Hz	BGD Hz keV^{-1}	Calib. source
Base	0	12				
^6Li	19	14	0.17	0.17	0.003	$\text{Mo K}\alpha$
^7Li	19	15	0.16	0.17	0.002	$\text{Mo K}\alpha$
^9Be	33	24	0.11	0.11	0.005	$^{137}\text{Cs} \rightarrow \text{Ba K}\alpha$
$^{10,11}\text{B}$	52	29	0.036	0.040	0.003	^{241}Am
^{12}C	75	~ 40	0.005	0.006	0.002	

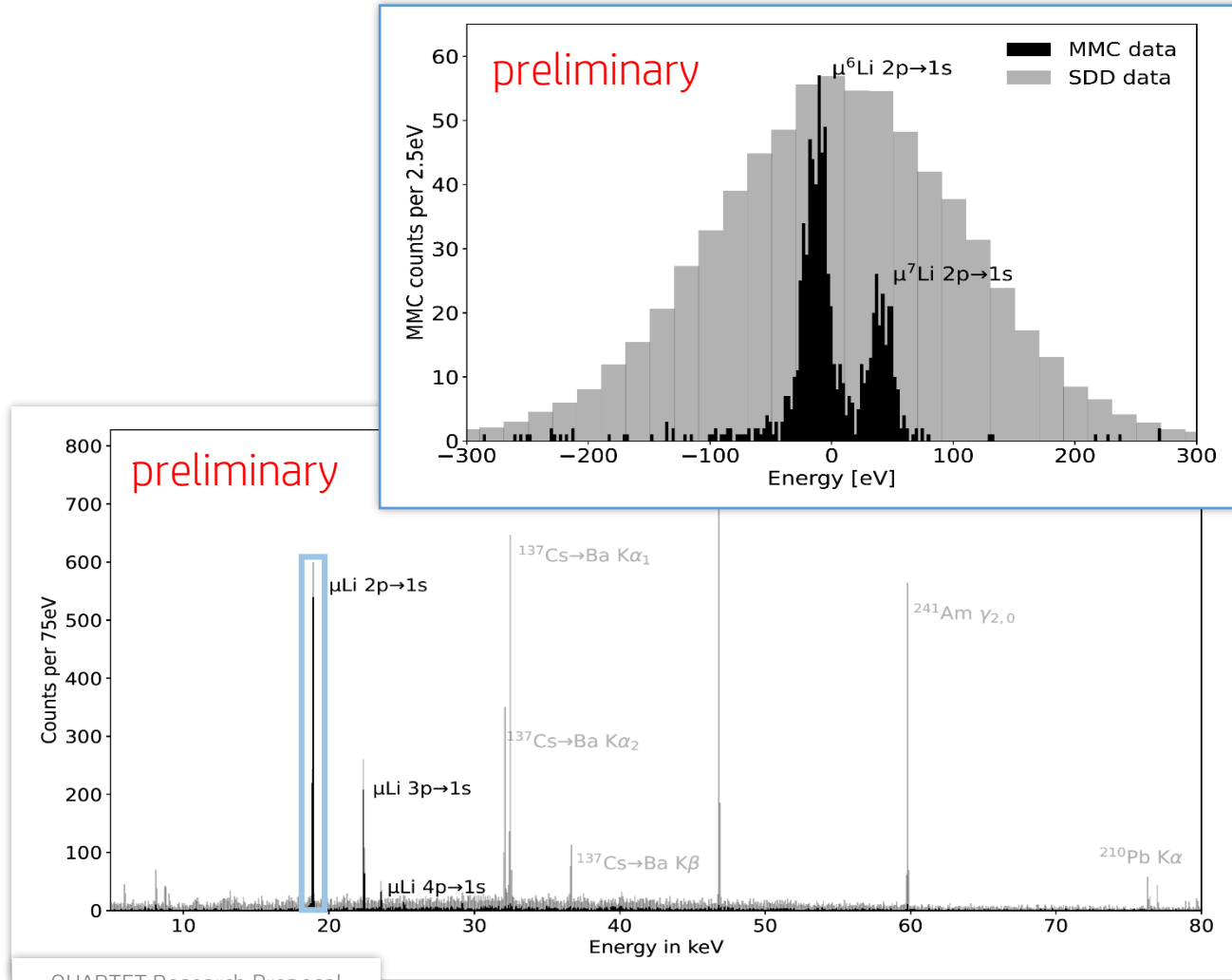
QUARTET – Open questions

- Investigate optimized calibration strategy over different energy ranges
- Compromise between energy resolution and quantum efficiency



Isotope shift of muonic
 ${}^6\text{Li}$ and ${}^7\text{Li}$ resolved !

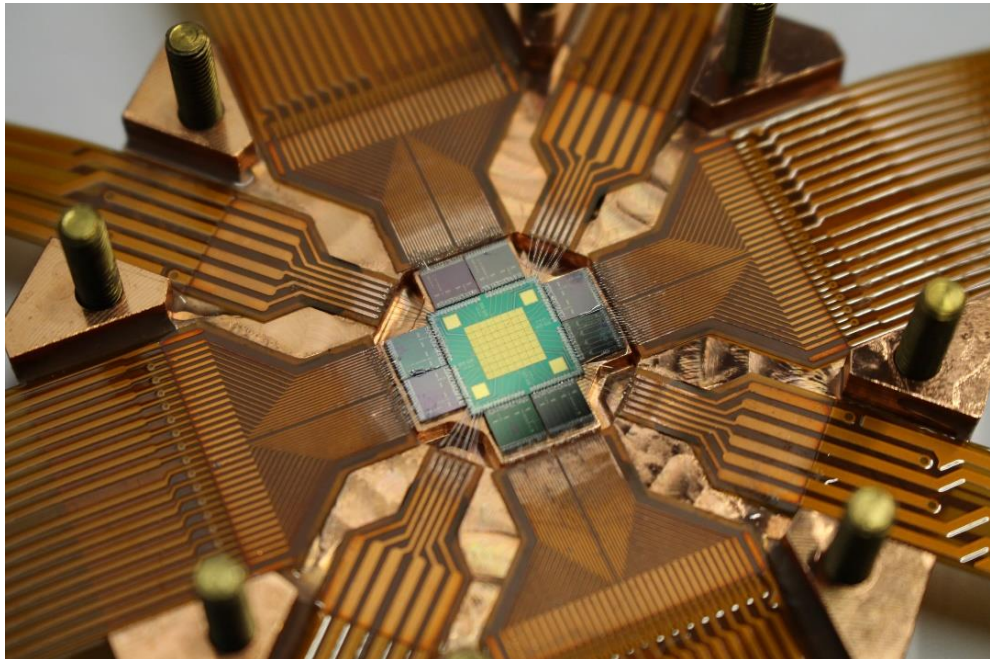
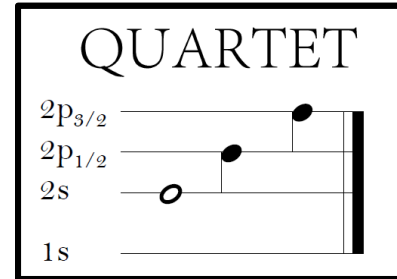
Target	$E_{2\text{p}-1\text{s}}$ keV	ΔE_{FWHM} eV	Rate Hz	Expected Hz	BGD Hz keV $^{-1}$	Calib. source
Base	0	12				
${}^6\text{Li}$	19	14	0.17	0.17	0.003	Mo K_α
${}^7\text{Li}$	19	15	0.16	0.17	0.002	Mo K_α
${}^9\text{Be}$	33	24	0.11	0.11	0.005	${}^{137}\text{Cs} \rightarrow \text{Ba } K_\alpha$
${}^{10,11}\text{B}$	52	29	0.036	0.040	0.003	${}^{241}\text{Am}$
${}^{12}\text{C}$	75	~ 40	0.005	0.006	0.002	



QUARTET – maXs-30 – Beamtime 2024

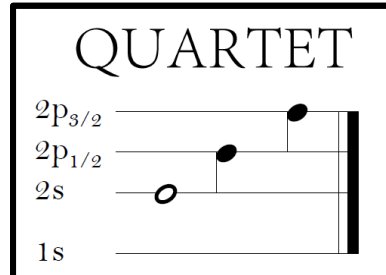
Goal: High precision spectroscopy of muonic Li, Be and B

Calibration strategy optimized for the different elements



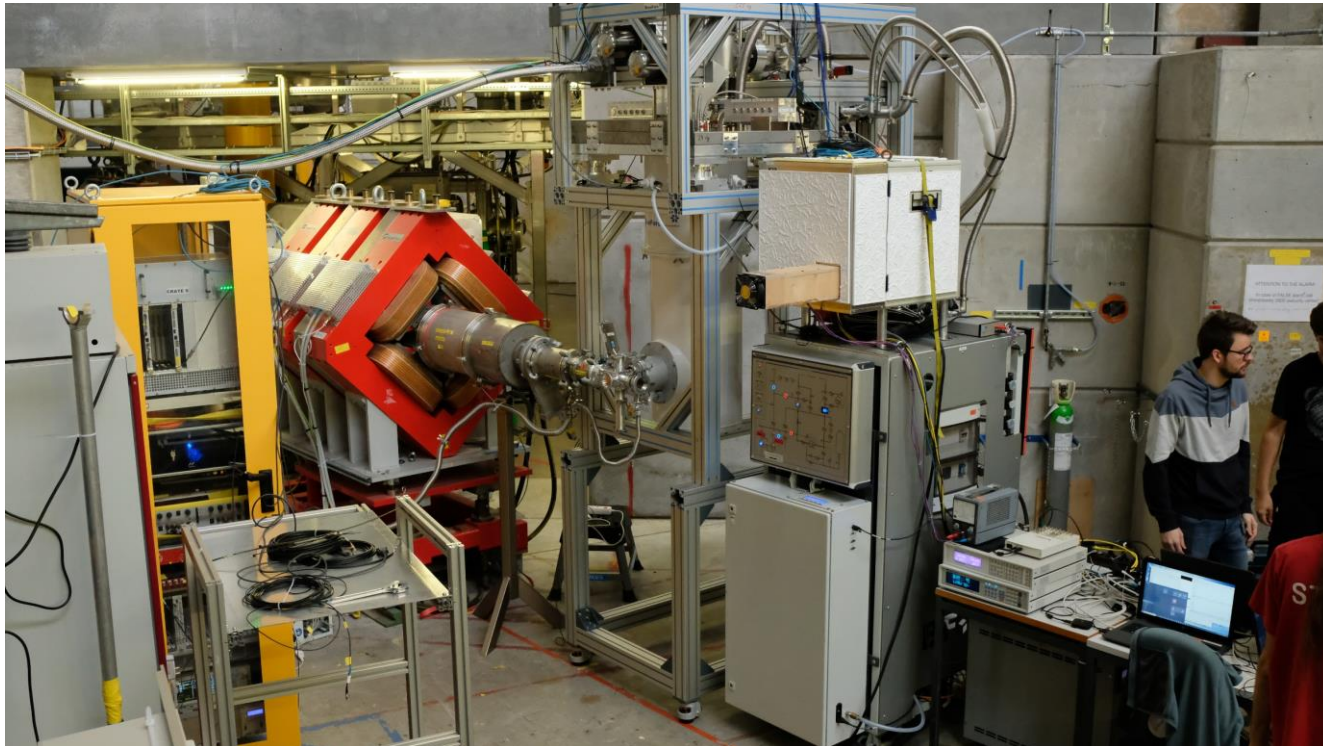
QUARTET – maXs-30 – Beamtime 2024

Goal: High precision spectroscopy of muonic Li, Be and B



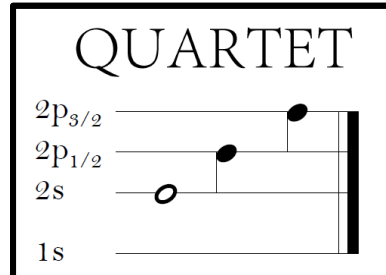
Calibration strategy optimized for the different elements

Detector system moved to PiE1 yesterday



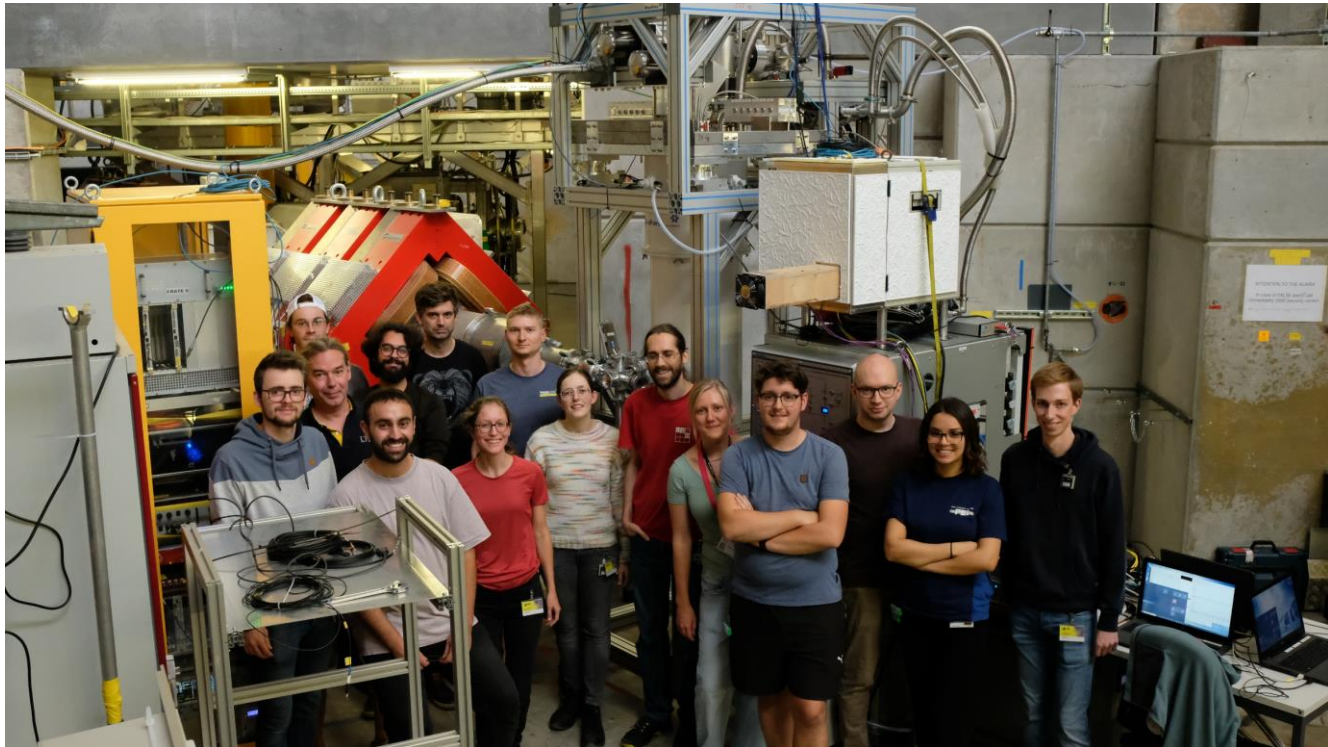
QUARTET – maXs-30 – Beamtime 2024

Goal: High precision spectroscopy of muonic Li, Be and B



Calibration strategy optimized for the different elements

Detector system moved to PiE1 yesterday



QUARTET – maXs-30 – Beamtime 2024

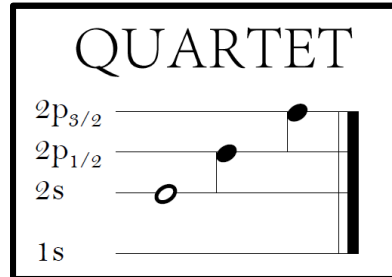
Goal: High precision spectroscopy of muonic Li, Be and B

Calibration strategy optimized for the different elements

Detector system moved to PiE1 yesterday



and we are excited to see the first photons tonight!



QUARTET – maXs-30 – Beamtime 2024

Goal: High precision spectroscopy of muonic Li, Be and B

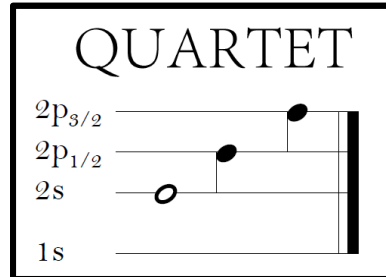
Calibration strategy optimized for the different elements

Detector system moved to PiE1 yesterday

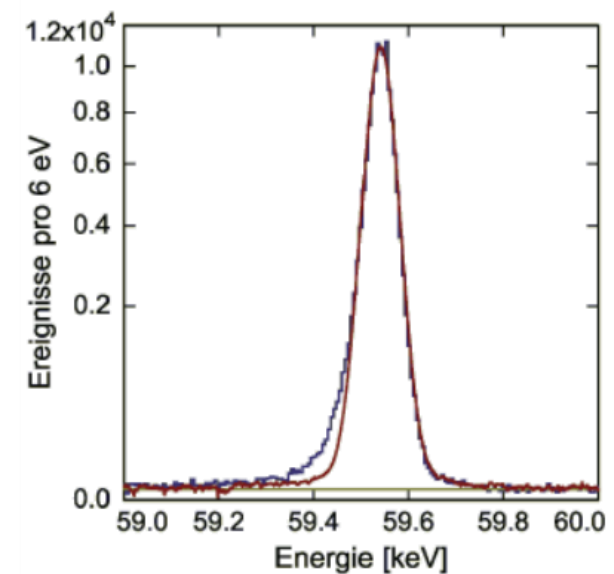


and we are excited to see the first photons tonight!

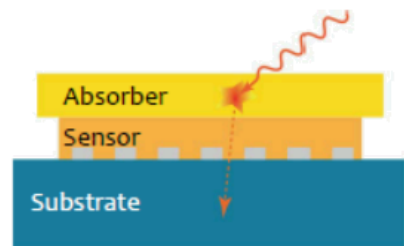
Thank you for
your attention!



Loss of athermal phonons to the substrate



Energy of athermal phonons
may be lost to substrate

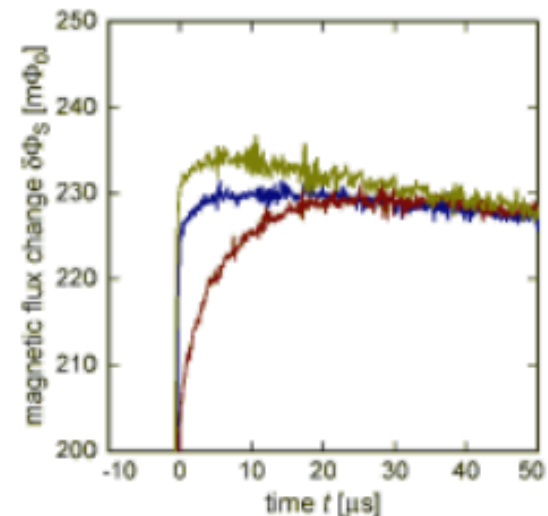
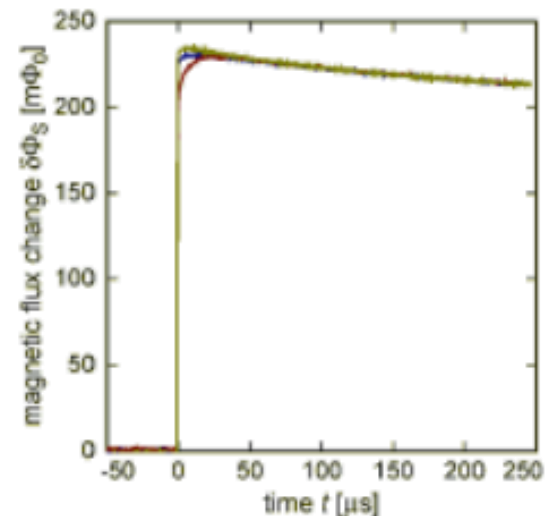


Stems reduce contact area
to a few percent



→ reduce contact area between sensor and absorber

In large absorbers: signal rise time limited by thermal diffusion



→ add thermal bottleneck between absorber and sensor

Challenge: remove heat from pixels in a closely packed array



Electroplate Au heat bath on front-side



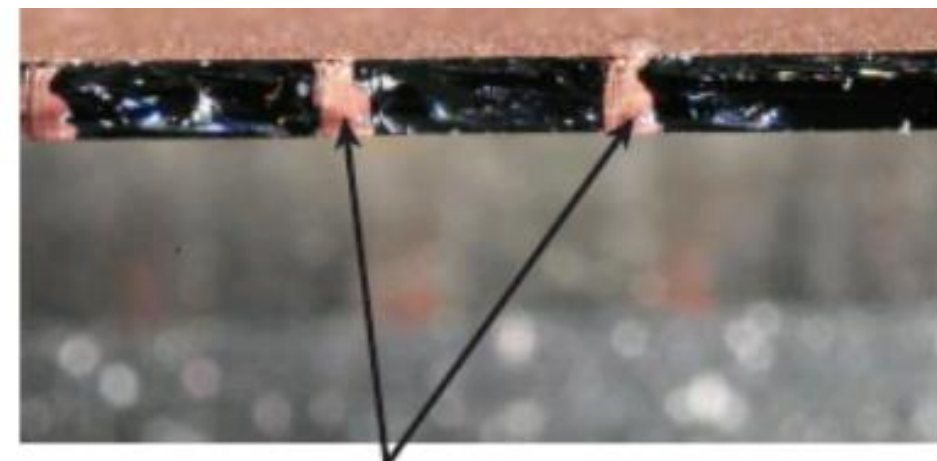
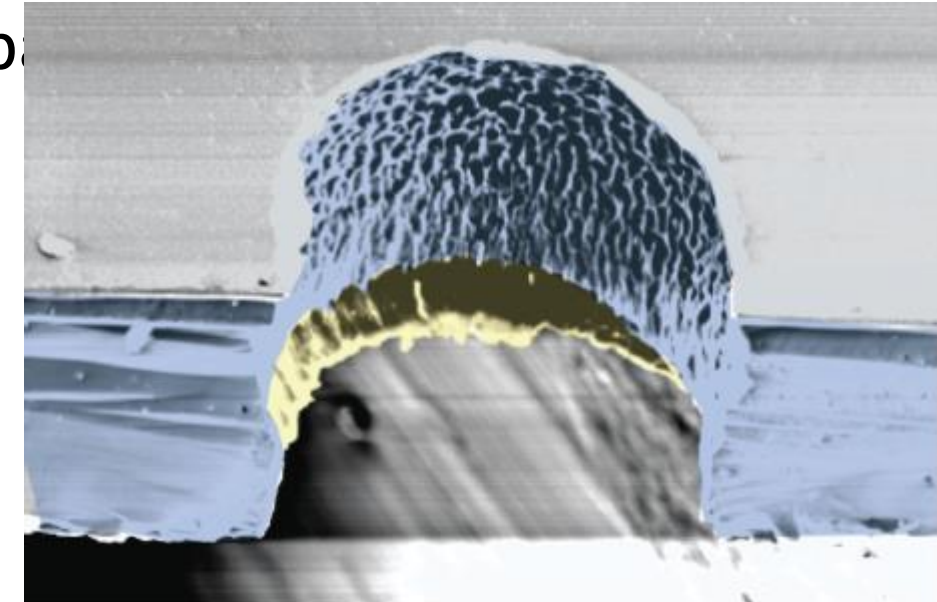
Au contact layer (FS) and etch mask (BS)



Bosch process from BS



Electroplate Cu on back-side



Completely filled TWV